Numerical Investigation of Water Loss Mechanisms During Hydraulic Fracturing Flow-Back Operation in Tight Oil Reservoirs

by

Mingyuan Wang

A thesis submitted in partial fulfillment of the requirements for the degree of

Master of Science

in

Petroleum Engineering

Department of Civil and Environmental Engineering
University of Alberta

Abstract

Multi-stage hydraulic fracturing is widely applied in tight reservoir exploitation. Production is enhanced significantly if hydraulic fractures can connect to regions with enhanced permeability due to the presence of micro (and induced) fractures. However, less than 50% of fracturing fluids are typically recovered. This study models the mechanisms of water loss and retention in fracture-matrix system. The effects of capillarity and geomechanics are systematically investigated, and the time scale of water imbibition under different reservoir conditions is tested. During the shut-in (soaking) and flow-back periods, the fracture conductivity decreases as effective stress increases due to imbibition. Previous works have addressed fracture closure during the production phase; however, the coupling of imbibition due to multiphase flow and stress-dependent fracture properties during shut-in is less understood. Numerical simulation results indicate the circumstances under which this phenomenon might be beneficial or detrimental to subsequent on tight oil production.

A series of mechanistic simulation models consisting of both hydraulic fractures and stochastically distributed micro fractures are constructed to simulate fluid distribution during shut-in and flow-back. Three systems: matrix, hydraulic fracture and micro fractures are explicitly represented in the computational domain. Fluid loss and retention mechanisms are systematically investigated in this study by subjecting mechanistic model to different reservoir conditions. Water imbibition into the matrix would help to displace hydrocarbons into nearby micro and hydraulic fractures, and this process could lead to an increase in initial rate. Although other water loss mechanisms including water loss in desiccated matrix and water trapping in induced micro fractures were proposed in literature, detailed understanding of the roles of water trapping in these systems is still lacking. Impacts of secondary fracture distributions and

properties, matrix permeability, multiphase flow functions, wettability, initial saturation, water injection rate and shut-in duration on fluid retention and the associated time scales are assessed. Increase in short-term oil production as a result of imbibition could be counteracted by the reduction in flow capability due to fracture closure. Therefore, the coupling of stress-dependent fracture conductivity and imbibition are studied next. Our results indicate that fracture compaction can enhance imbibition and water loss, which in turn leads to further reduction in fracture pressure and conductivity. Spatial variability in micro-fracture properties is also modeled probabilistically to investigate whether it is possible for fracturing fluid to be trapped in the micro fractures, or conversely, the micro fractures could provide alternate pathways for fluids to access the hydraulic fracture systems.

This work presents a quantitative study of the controlling factors of water retention due to fluid-rock properties and geomechanics. It investigates the roles of multi-scale fractures in flow-back behavior and ensuing recovery performance. The results highlight 1) the crucial interplay between shut-in duration and properties of connected fractures in short- and long-term production performances; 2) the critical interaction between imbibition and geomechanics in short- and long-term production performances. The results would have considerable impacts on understanding and improving current industry practice on fracturing design and assessment of stimulated reservoir volume.

Preface

This thesis is an original work by Mingyuan Wang. No part of this thesis has been previously published.

Dedicated to my parents and all my family members for their love, endless support and encouragement.

Acknowledgements

First and foremost, I would like to express my sincere appreciation to Dr. Juliana Leung for her encouragement and support through my study and research. This work would not have been possible without her continued guidance, unlimited patience and insightful ideas during the entire research. I am also grateful to Dr. Hassan Dehghanpour and Dr. Huazhou Li for coming to my final defense as examining committee members and giving me constructive comments and feedbacks.

I would like to thank all the professors for providing me with the solid knowledge and cutting-edge technologies of petroleum engineering. I also want to thank all the members in Dr. Leung's research group who helped and inspired me through different problems, and I would like to thank all the people who helped me during my MSc.

My gratitude also goes to University of Alberta for providing the financial support. I would also like to thank the Computer Modeling Group Ltd. (CMG) for providing the academic licenses for IMEX.

Finally, I am truly grateful to my family, for their live, endless support and encouragement.

Table of Contents

List of Tables

List of Figures

List of Symbols

A_M = Contact area between fracture and matrix m^2

a_F = Fracture aperture m

a_{NF} = Secondary-fracture aperture m

a_{HF} = Hydraulic-fracture aperture m

B_o = Formation volume factor of oil m^2/m^2

B_w = Formation volume factor of water m^2/m^2

BHP = Bottom-hole pressure Pa

C_t = Total compressibility Pa^{-1}

E = Young's modulus Pa

F_{cd} = Normalized fracture conductivity

P = Probability

P_b = Bubble point pressure Pa

P_c = Capillary pressure Pa

P_{cM} = Capillary pressure in matrix Pa

P_{cF} = Capillary pressure in fracture Pa

P_{cow} = Capillary pressure of water-oil system Pa

P_{cog} = Capillary pressure of oil-gas system Pa

P_i = Initial reservoir pressure Pa

P_{wf} = Minimum wellbore flowing pressure Pa

J = Leverett j function

k_M = Matrix permeability m^2

k_{NF} = Secondary-fracture permeability m^2

k_{HF} = Hydraulic-fracture permeability m^2

n = Index of refined grid

N = Total number of refined grids

N_{Ca} = Capillary number

N_F = Total number of secondary fracture in the domain

SRV = Simulated reservoir volume

S_{wM} = Matrix water saturation

S_{wNF} = Secondary fracture water saturation

S_{wHF} = Hydraulic-fracture water saturation

S_{wi} = Initial water saturation

S_{wirr} = Irreducible water saturation

P_{32} = Fracture intensity

P_j = Pressure of phase *j* Pa

P_F = Water pressure in fracture Pa

P_M = Water pressure in matrix Pa

P_{Fi} = Initial water pressure in fracture Pa

u_j = Flow rate of phase *j* m/s

q_{oi} = Initial oil flow rate m^3/day

q_{inj} = Water injection rate during injection period m^3/day

Q_o = Cumulative oil production m^3

Q_w = Cumulative water production m^3

R_s = Solution gas oil ratio m3/m3

RC = Reservoir condition

SC = Surface condition

v = flow rate m/s

V_{PF} = Pore volume in fracture m^3

t_{inj} = Water injection duration hr

T = Transmissibility

w = Distance from a particular refined grid outer boundary to the parent grid center m

w_e = Half width of the parent grid m

Greek Symbols

∇ = Gradient *m-1*

μ' = Viscosity *Pa•s*

μ = Mean of probability distribution

σ = Standard deviation of probability distribution

σ' = Interfacial tension between water and oil N/m

σ_c = Closure stress for hydraulic fractures Pa

σ_c' = Closure stress for secondary fractures Pa

ϕ_M = Matrix porosity

ϕ_{NF} = Secondary fracture porosity

ϕ_{HF} = Hydraulic-fracture porosity

λrj = Relative mobility of phase j

Chapter 1: Introduction

This chapter presents the background of unconventional resources, introduction to hydraulic fracturing and flow-back operation, problem statement, research objective and thesis outline.

1.1 Background

With declining conventional petroleum resources, exploration and exploitation of unconventional resources, including tight-sandstone oil/gas, shale oil/gas, coalbed methane, gas hydrate and heavy oil, are becoming more important (Zou 2012).

In recent year, tight oil reservoirs are gaining much attention in North America. Compared with conventional resources, unconventional reservoirs have their unique characteristics. Sandstone and limestone are common lithologies for tight oil reservoir (Zou 2012). Tight oil reservoirs have very low matrix porosity and permeability due to its fine-grained sandstones and micro-scale pore structure (Pitman *et al*., 2001). For example, in Bakken formation, its porosity ranges from 0.01 to 0.16, averaging about 0.05, and its permeability ranges from 0 to 20mD, averaging 0.04mD (Pitman *et al*., 2001). Capillary pressure in tight reservoir can be very high due to its low permeability (Holditch *et al*., 1979). Besides, tight reservoirs usually have relatively developed natural fractures networks (Pitman *et al*., 2001).

Low fluid mobility in tight reservoirs is the main challenge for economic tight oil recovery. Due to the breakthrough of horizontal drilling and hydraulic fracturing technologies in recently years, economic production of tight oil became possible. Many tight oil reservoirs, such as the Bakken

tight oil reservoir and the Eagle Ford tight oil reservoir are explored and exploited in North America. Significant production has been reported from these reservoirs, e.g. production in the Bakken tight oil reservoir has reached 1230×10^4 t in 2009 (Zou 2012).

Hydraulic fracturing technique would accelerate production and increases reserves significantly if artificial fractures can connect to sweet spots with enhanced permeability due to the presence of secondary fractures (Zou 2012; Pitman *et al*., 2001). In some instances, hydraulic fracturing may reactivate secondary fractures that are closed under initial in-situ stress conditions or induce additional ones near the wellbore.

1.2 Hydraulic Fracturing in Unconventional Tight Reservoirs

Since the early fifties, hydraulic fracturing has been adopted commercially (Fjar *et al*., 2008; King 2012). By the late 1970s, horizontal wells were widely used (King 2012). In recent years, hydraulic fractured horizontal wells are widely used to exploit tight reservoirs.

During hydraulic fracturing operation, there are three phases, fracturing fluid injection phase, shut-in (soaking) period and flow back period (McClure 2013; McClure 2014).

During injection period, thousands of cubic meters of fracturing fluid are injected into the formation (McClure 2014). In tight oil reservoir, slick water is typically used as fracturing fluid (Mayerhofer et al., 1998; Reinicke et al., 2010). During the injection phase, fractures initiate and propagate (Fjar *et al*., 2008). Water may leak of into the matrix, resulting in a fracturing fluid efficiency (fracturing fluid volume in fracture over total injected volume) to be less than 100% (Economides *et al*., 2000). The fracture pattern is influenced by reservoir properties, such as reservoir permeability, relative magnitude between the maximum horizontal stress and the

minimum horizontal stress (Pak 1997). Hydraulic fracture network typically exists as a cluster of smaller planes rather than a single plane (King 2012). Besides, the existence of natural fractures and induced secondary fractures could also contribute to the generation of complex fracture network when artificial fracture is connected with natural fractures (King 2012). Micro-seismic data can be used as an indication for fracture propagation (Fisher *et al*., 2002).

After injection period, the well is shut-in for a period, and the fluid pressure immediately after injection is approximately the Initial Shut-in Pressure (ISIP) (McClure 2013). According to micro-frac investigations in western Canadian tight oil reservoirs, including Viking Sandstone and Cardium Sandstone, the value of ISIP is typically higher than the initial reservoir pressure by 15 to 55 MPa (Woodland *et al*., 1989). During the shut-in period, fracturing fluid and oil redistribute among the fracture and matrix systems under complex interplay between capillary and viscous forces, and the induced fractures would gradually close as the fracture effective stress increases (Economides *et al*., 2000). Field observations indicate that shut-in period has significant influence on short-term and long-term oil production, which could be beneficial or detrimental (Crafton 2010).

The fracturing fluid begins to flow back as the well resumes production (McClure 2014). According to Crafton (2010), "flow back" refers to the few hours to weeks of production immediately after shut-in period. However, less than 50% of fracturing fluids are typically recovered (McClure 2014; Cheng 2012; Wattenbarger *et al*., 2013; Makhanov *et al*., 2014). Evidence indicates that flow back operation can influence long term production and hydrocarbon recovery (Crafton 2008, 2010). Therefore, hydraulic fracturing flow back operation strategy should be optimized based on reservoir rock-fluid properties.

1.3 Problem Statement

During the flow-back operation, it is often reported that only 10-50% of the fracturing fluids ca be recovered. Imbibition plays an important role in water loss due to high capillary pressure in tight reservoirs. As more water imbibed into the matrix, water saturation in the matrix increases, which can cause oil relative permeability decreases and thus reduce oil production. However, many field observations indicate that extended soaking period can lead to higher short-term oil production (Cheng 2012; Ghanbari *et al*., 2013). Therefore, whether water imbibition will be beneficial or detrimental to subsequent oil production should be investigated.

In addition to capillary effect, geomechanics effect can also cause water loss. During the shut-in (soaking) and flow-back periods, the fracture conductivity decreases as effective stress increases due to imbibition. This reduced fracture conductivity could cause additional water loss. Therefore, the coupling effect of stress-dependent fracture conductivity and imbibition should be studied.

Besides, different reservoir properties could also influence water loss, such as fracture network properties, initial water saturation, multiphase flow functions, etc. Spatial variability in micro-fracture properties should also be modeled probabilistically to investigate the impact of fracture network heterogeneity on water loss mechanisms and oil production.

Furthermore, because shut-in period and flow back operation can significantly impact production performance, hydraulic fracturing flow back operation should be optimized according to different reservoir properties, including shut-in time and flow back bottom-hole pressure.

1.4 Research Objectives

The objective of this research is to investigate different water loss mechanisms, their influence on subsequent oil production and provide fracturing flow back operational strategy by using numerical simulation method, which entails:

(1) Conduct a series of mechanistic models that take into consideration factors such as water injection rate or ISIP, secondary fracture capillary pressure, secondary fracture heterogeneity, formation desiccation, wettability, initial water saturation and solution gas.

(2) Quantify the multiphase fluid distribution and trapping during shut-in in fractured tight rocks due to both matrix imbibition and water retention in secondary fractures.

(3) Study the impacts of secondary fracture properties and multiphase functions on these retention mechanisms.

(4) Incorporate stress-dependent fracture conductivity on imbibition and flow-back modeling.

(5) Investigate the influence of various operational strategies on short-term and long-term production.

Since the origin of fracturing fluid loss in unconventional reservoirs remains a widely-debated subject among practitioners, results obtained from this study would provide explanations regarding the possible mechanisms of fluid loss and offer insights for optimizing operational strategies.

1.5 Thesis Outline

This thesis consists of six chapters. The outline of these chapters is provided as follows:

Chapter 1 presents the introduction to unconventional reservoir and hydraulic fracturing. Problem statement and research objective are also presented in this chapter.

Chapter 2 presents the literature review including the existing investigation on water loss mechanisms and flow back strategy.

Chapter 3 presents the methodology used in this study including mechanistic numerical model construction, discrete fracture network, local grid refinement and stress dependent fracture conductivity.

Chapter 4 presents the numerical investigation on the impact of secondary fracture distributions and properties, matrix permeability, multiphase flow functions, initial saturation, water injection rate and shut-in duration on fluid retention and associated time scales.

Chapter 5 presents the numerical investigation on the impact of wettability, stress dependent fracture conductivity and disconnected secondary fracture network.

Chapter 6 presents the conclusions and recommendations.

Chapter 2: Literature Review

In this chapter, the literatures about water loss mechanisms, experimental, analytical and numerical simulation studies are reviewed.

2.1 Water Loss Mechanisms

Various fluid-loss mechanisms have been reported in the literature (Pagels et al., 2012; Wattenbarger et al., 2013). Water imbibition from fracture system into rock matrix is facilitated by high matrix capillary pressure in tight rocks. Water and oil redistribute in the fracture-matrix system during this counter-current imbibition process. (Pagels et al., 2012; Bahrami et al., 2012; Holditch et al., 1979; Makhanov et al., 2014; Fakcharoenphol et al., 2013; Fan et al., 2010; Cheng 2012; Wattenbarger et al., 2013). Besides matrix imbibition, water can be retained in secondary fractures (Pagels et al., 2012; Fan et al., 2010). Geomechanics also plays a role in low water recovery because of fracture compaction during the shut-in and flow-back periods (McClure, 2014; Ehlig-Economides et al., 2012). Under certain circumstances, induced micro fractures may lose contact with the main hydraulic fracture system (Pagels et al., 2012). In addition, gravity segregation in hydraulic fractures can also contribute to low water recovery (Parmar et al., 2012, 2013; Ghanbari, 2015; Ghanbari and Dehghanpour, 2016).

2.2 Field Observation

2.2.1 Flow-back Data and Fracture Intensity

Flow-back data from Horn River Basin has been analyzed to obtain fracture properties

(Zolfaghari et al., 2015; Ghanbari and Dehghanpour, 2016). According to the volumetric analysis (Ghanbari and Dehghanpour, 2016), relationship between early time flow-back efficiency and cumulative gas recovery can be used to categorize producing wells into two groups: 1) wells with high gas production and low water recovery; 2) wells with low gas production and high water recovery. Wells with high gas production and low water recovery result from enhanced counter-current imbibition and water retention in secondary fractures in more complex fracture network, while wells with low gas production and high water recovery can be attributed to less complex fracture network. This hypothesis has been confirmed by flow-back salt-concentration transient study (Zolfaghari et al., 2015). According to the mathematical model presented by Zolfaghari et al. (2015), the fracture network complexity can be reflected from the flow-back salinity and load recovery profile. They concluded that as for more complex fracture network, salinity constantly increases with load recovery, while as for less complex fracture network, salt concentration initially increases and then a plateau is reached.

2.2.2 Impact of Shut-in Duration

As an important operational procedure in hydraulic fracturing operation, the impact of shut-in duration can be beneficial or detrimental for subsequent hydrocarbon production. Field observation from the Marcellus formation is presented in Cheng (2012). The well experienced a short flow-back period after fracturing fluid injection period, and the well is shut in subsequently. The initial gas flow rate was enhanced significantly after the shut-in period with lower water recovery. Fan et al. (2010) also proposed that higher initial production rate could often be associated with low water recovery.

However, Crafton et al. (2013) analysed 270 wells (including wells from the Marcellus formation) and concluded that shut-in duration can be detrimental. Their results also indicated

that there was no obvious relationship between the length of shut-in duration and the degree of its adverse effect. The drawback of this study is that though these wells have been shut in for different durations, they also exhibit different reservoir rock/fluid properties. In other words, despite of the differences in production and water recovery profiles between two nearby wells, it is difficult to attribute these differences exclusively to the impacts of shut-in duration, since the effects of reservoir heterogeneities could not be precisely quantified. Therefore, clear understanding regarding the impact of shut-in duration is not readily available from field observations.

2.3 Experimental, analytical and numerical studies

Experimental, analytical and numerical simulation studies of imbibition and flow-back process in fractured media have been published. Brownscombe et al. (1952) performed a series of countercurrent spontaneous imbibition experiments and concluded that large fracture system would provide a conductive system enhancing the imbibition process. Makhanov et al. (2012) observed that imbibition rate is higher when imbibition direction is along the bedding plane. Makhanov et al. (2014) demonstrated that spontaneous imbibition rate in tight rocks would depend on factors including clay content, properties of secondary fractures, shut-in duration, and matrix mineralogy. Imbibition experimental results from Fakcharoenphol et al. (2014) indicate that low-salinity brine has higher imbibition rate compared with high-salinity brine due to osmotic effect. Ghanbari et al. (2014a, b) concluded that 1) shale pore network is more water wet and its rock mass is more oil wet; 2) water imbibition rate is reduced with higher initial water saturation; 3) microfractures can be generated due to soaking in shale. Imbibed water in the

matrix could also cause water blockage and have adverse effect on oil/gas relative permeability, which has been demonstrated by various experimental studies (Bazin et al., 2010; Dutta et al., 2014). Longoria et al. (2015) indicated that water can be dissipated deeper into the matrix during shut-in. Liang et al. (2015a) also demonstrated that imbibition during shut-in can mitigate the impact of water block and reduced hydrocarbon relative permeability caused by capillary end effect. However, this mitigation is temporary because during flow-back, water will accumulate in the matrix near fracture face and cause blockage due to capillary discontinuity (Liang et al., 2015a). Liang et al. (2015 a, b) and Longoria et al. (2015a) demonstrated that surfactants can help clean water blockage and enhance hydrocarbon relative permeability.

Besides imbibition, the effect of gravity segregation has been investigated by experiments. Parmar et al. (2012, 2013) investigated the impact of gravity on fracturing fluid recovery by experimental method and the results indicate that when the flow direction is opposite from gravity direction, water recovery from hydraulic fractures can be very low due to unstable displacement; therefore, large quantity of water will be retained in the bottom of fractures. This conclusion has been confirmed by numerical simulation results from Ghanbari and Dehghanpour (2016).

(Semi)-analytical models, which are essentially simplified solutions to the detailed governing equations, have been employed extensively in the areas of pressure transient (PTA) and rate transient (RTA) analysis. Recent works have extended their formulations to analyze early-time flow-back production data for fracture characterization (Clarkson et al., 2013; Alkouh et al., 2014; Williams-Kovacs et al., 2013; Ezulike et al., 2014; Adefidipe et al., 2014). However, these techniques have limited application in understanding water retention and imbibition mechanisms for a number of reasons: (1) assumptions associated with these models involve homogeneous

fracture properties and sequential depletion from matrix to secondary fractures and from secondary fractures to hydraulic fracture in a fully-connected fracture network, failing to capture the impacts of realistic fracture networks on water loss and multiphase production during flow-back (Al-Ahmadi 2010); (2) certain studies presume that water is immobile within the secondary fracture network (Williams-Kovacs et al., 2013); and (3) capability to incorporate multiphase flow functions (relative permeability and capillary pressure) in matrix and fracture systems are limited. For example, Abbasi et al. (2014) assumed single-phase flow, although two phase flow might exist even during early flow-back. Ezulike et al. (2013) proposed a two-phase dual-porosity model with single-phase oil flow in matrix and negligible saturation and capillary pressure gradient in fracture, assuming that the initial hydrocarbon volume in fracture prior to flow-back was known. It is clear that none of these models are suitable for studying fluid-loss mechanisms in complex fractured media because two-phase flow and fluid distribution during shut-in and flow-back are not taken into account explicitly.

On the contrary, the complex physics of fluid flow in fractured porous media can be captured by numerical simulation. Three approaches have been developed for numerically simulating fluid flow in fractured media. In the single-porosity approach, matrix and fractures systems are explicitly represented in the computational domain. High permeability and porosity values are assigned to fracture cells. Flow in fracture-fracture, matrix-fracture, matrix-matrix connections are simulated in detail (Karimi-Fard et al., 2004; Aziz et al., 1979; Qasem et al., 2008; Rubin 2010). The second approach is the continuum approach, which replaces a multiple-porosity system with an equivalent medium consists of continuous properties. One example is the dual-porosity dual-permeability approach (Warren et al., 1963). A third approach such as the triple-porosity model can be considered as a combination of the first and second approaches, in which

flow within the connected fracture network is modeled explicitly, while matrix contribution is modeled through a set of transfer functions. To explicitly compute saturation variation and water retention in both matrix and fracture systems, only the single-porosity approach has been adopted successfully (Cheng 2012; Wattenbarger et al., 2013).

Cheng (2012) built a single-porosity model incorporating eight stages of hydraulic fractures, with symmetrical and fully-connected secondary fractures. Capillary pressure was assigned in matrix cells, while capillary pressure was ignored in fracture cells in a gas reservoir. Impacts of extended shut-in, capillary pressure and relative permeability functions, and permeability damage on the dynamics of gas-water distribution were studied. It was demonstrated that water imbibition driven by capillarity would control water-gas redistribution in matrix-fracture system during shut-in period and lead to an increased initial flow rate. Fakcharoenphol et al. (2013) built a triple-porosity model of a bi-wing hydraulic fracture connected to a secondary fracture-matrix network consisting of a continuum of interconnected network and imbedded organic and non-organic matrix. High matrix capillary pressure and small secondary fracture capillary pressure were used in the model. They demonstrated that early gas rate would increase after extended shut-in due to water imbibition under capillarity, osmotic effect, and gravity. Cheng (2012) and Fakcharoenphol et al. (2013) both observed that there is no long-term production benefit from extended shut-in duration. In Wattenbarger et al. (2013), a single-porosity model of a multi-hydraulically fractured horizontal well and symmetrical, fully-connected secondary fractures were used. Identical capillary pressure and relative permeability functions were assumed in matrix and secondary fractures. A number of concepts including capillary pressure, relative permeability, permeability jail (neither wetting nor non-wetting phase could flow over a particular saturation range), aperture and spacing of hydraulic and secondary fractures, and shut-

in duration were investigated. Their conclusions were 1) lower relative permeability in both matrix and secondary fractures would reduce imbibition rate, causing water saturation to increase in natural fractures during shut-in; 2) higher matrix capillary pressure can enhance imbibition; 3) water retention in natural fractures increases with fracture width and intensity; 4) Permeability jail in both matrix and secondary fractures would also increase water saturation in natural fracture with an adverse effect on production. Ghanbari (2015) and Ghanbari and Dehghanpour (2016) constructed a single-porosity model with hydraulic fracture and symmetrical, fully connected secondary fractures. They investigated the impact of gravity segregation, shut-in duration, secondary fracture density and matrix capillary pressure. They concluded that 1) increasing shut-in duration can benefit short-term gas production and reduce water recovery; 2) higher capillary pressure can result in lower water recovery and lower long-term gas production because of water blockage; 3) increased fracture complexity results in higher gas production and lower water recovery.

2.4 Drawbacks in existing numerical investigation

A main drawback of these previous studies is the assumption of symmetrical and fully-connected secondary fracture network, as it fails to capture the heterogeneity commonly observed in unconventional reservoirs. Therefore, stochastic discrete fracture networks are adopted in this study to capture the complexity and heterogeneity of fracture systems, enhancing statistical assessment of their impact on flow performance and uncertainty assessment. Various formation evaluation techniques and geostatistical methods can be used to infer fracture network special statistics (Qasem et al., 2008). Discrete fracture method has been successfully used in modeling fluid flow in fractured porous media by randomly generating fractures according to statistical

distribution of fracture parameters (Long et al., 1985; Cacas et al., 1990; Xia et al., 2014; Wang and Leung 2014, 2015). Probability distributions derived from geostatistical study are used for fracture parameter sampling (e.g. length, spacing and aperture) (Baecher et al., 1977; Rouleau et al., 1985; Gale et al., 1991). Fracture spacing is defined in 1-D fracture distribution, while for 2-D, fracture intensity is adopted to represent the degree of fracture abundance (Chilès 1988). These discrete fracture networks are subsequently discretized and single-porosity simulations are performed.

Another issue associated with the aforementioned studies is the assignment of multiphase flow functions in the fracture systems. Firoozabadi et al. (1990) have demonstrated that fracture capillary pressure is greater than zero, depending on the roughness, aperture, and pore structure. This is inconsistent with Cheng (2012), in which zero secondary fracture capillary pressure was used, and Wattenbarger et al. (2013), in which secondary fracture capillary pressure was the same as matrix capillary pressure. In addition, wettability influence has often been ignored: assuming neural wettability and identical relative permeability functions in both matrix and secondary fractures (Wattenbarger et al., 2013). Furthermore, the influence of ISIP was often ignored.

Although matrix imbibition has been studied rather extensively, detailed understanding of numerous aspects is still lacking. First, in terms of secondary fracture trapping, Pagels et al. (2012) and Fan et al. (2010) proposed that water could be retained in the small secondary fractures due to their large capillary pressure, but this claim was not substantiated with physical evidence or modeling results. Wattenbarger et al. (2013) demonstrated that low relative permeability in matrix and fracture, high fracture width, and strong permeability jail in matrix and fracture would increase water retention in secondary fracture during shut-in. However,

detailed sensitivity analysis of various controlling factors (e.g., secondary-fracture permeability and capillary pressure) has not been presented. Second, the influence of matrix desiccation such as that in the Cardium formation (Purvis et al., 1979; Lamson et al., 2013) is not well understood. Third, complex interplay of viscous forces and capillary forces and their influences on both matrix imbibition and secondary fracture retention are not fully investigated. Finally, field observation reveals that shut-in duration has a significant impact, either adverse or beneficial, on short-term and long-term production (Crafton, 2010). Although Cheng (2012) and Fakcharoenphol et al. (2013) have reported an increased initial gas flow rate as a result of extended shut-in, time-scale analysis for all fluid-loss mechanisms is still not well understood.

Although investigation of individual impacts of relative permeability and capillary pressure functions has provided important insights, the role of matrix wettability in counter-current imbibition in tight formations is less understood. Degree of wettability can be reflected by coupling of relative permeability, capillary pressure function and initial water saturation (Anderson 1987a, 1987b). As the matrix becomes more water wet, capillary pressure and oil relative permeability increase, while water relative permeability decreases, resulting in an increase in initial water saturation (Peters 2012; Dandekar 2013; Jadhunandan et al., 1995; Bennion et al., 2002; Jerauld et al., 1997). Experimental results by Morrow et al. (1978) indicated that imbibition rate would increase with water wettability. Takahashi et al. (2009) also observed that water did not imbibe spontaneously into the matrix that was intermediate to strongly oil-wet, and imbibition was enhanced under water-wet condition. Blair et al. (1960) demonstrated with numerical simulations that as oil relative permeability increased and water relative permeability decreased (i.e., formation becoming more water wet), an increase in oil production due to enhanced counter-current imbibition was observed. A similar conclusion was

presented by Almulhim et al. (2014), who simulated a dual-permeability gas-water formation with hydraulic fracture, secondary fracture and matrix systems. However, none of these works have discussed the effects of initial water saturation corresponding to changes in wettability.

Findings from various previous studies regarding the specific influence of initial water saturation on imbibition are inconclusive (Li et al., 2006; Li et al., 2014). Blair (1960) concluded from core-scale numerical simulation models that as initial water saturation decreased, imbibition rate and oil production increased. However, experiments results from Cil et al. (1998) demonstrated that high initial water saturation (> 0.2) was positively related to oil recovery (a trend that is opposite to that presented by Blair (1960), while low initial water saturation (< 0.2) had no significant impact on oil recovery. Zhou et al. (2000) and Tong et al. (2002) also observed from experimental results that as initial water saturation decreased, imbibition rate and final oil recovery would decrease. However, these studies do not involve fractured rocks. Karimaie et al. (2007) reported that as initial water saturation increased, oil rate and final recovery in fractured carbonate rocks would increase. In order to reconcile this discrepancy regarding the impact of initial water saturation on imbibition, Tang et al. (2001) conducted experiments under varying wettability condition and showed that for strongly water-wet condition, oil recovery would decrease with initial water saturation, while for weakly or intermediate water-wet conditions, an opposite trend was observed. Li et al. (2006) attributed this discrepancy to the inconsistent definitions of hydrocarbons recovery and imbibition rate employed in various studies. Li et al. (2014) demonstrated with an analytical model that oil recovery was controlled by the coupling of wettability, initial water saturation, capillary pressure and relative permeability functions. Unfortunately, their study did not incorporate fracture networks. It is clear that the coupled effect of multiphase flow functions and initial water saturation as a function of wettability on

imbibition in unconventional reservoirs, where fractures are observed at multiple scales, is not fully understood.

Stress-dependent fracture conductivity is another important factor controlling water recovery. Decrease in propped/hydraulic fracture conductivity can result from proppant fine generation and migration (Pope et al., 2009), proppant crushing in harder rock and proppant embedment in softer rock (Fan et al., 2010). Hydraulic fracture conductivity also decreases as fluid pressure inside the fracture decreases. Closure stress refers to the effective stress inside the fracture and is defined as the difference between the in-situ stress perpendicular the fracture and the pressure inside the fracture (Yu et al., 2014). Alramahi et al. (2012) measured the effect of closure stress on propped fracture conductivity, and the results indicated that formations with different stiffness (i.e. different Young's modulus) would exhibit different stress-dependent fracture conductivity relationships. Experimental results in Huo et al. (2014) also illustrated that increasing effective stress could reduce fracture aperture and permeability. According to the stress-dependent micro-fracture conductivity measurements for a set of middle Bakken tight oil core samples in Cho et al. (2013), secondary fractures are commonly regarded as weakly propped, since the cementing minerals and surface roughness can retain permeability when the fluid pressure drops.

The impact of stress-dependent fracture conductivity on flow-back has been the focus of recent research efforts. An early numerical study by Sherman et al. (1991) investigated the impact of operating procedures on fracturing fluid recovery and productivity of a hydraulically-fractured gas well, and their results indicated that rapid fracture closure due to sharply decreasing bottom-hole pressure could trap fracturing fluid and reduce gas production. Ehlig-Economides et al. (2012) postulated that the closure of induced secondary fractures during flow-back could cause water-filled micro fractures to lose contact with the main hydraulic fracture, leading to an

increased water loss. Osholake et al. (2013) employed numerical simulations to model the impact of proppant crushing and operational conditions on gas production. They concluded that 1) proppant crushing reduces gas production; 2) reducing bottom-hole pressure would improve water and gas production (Osholake et al., 2013); this observation is inconsistent with the results from Sherman et al. (1991). Yu et al. (2014) performed history matching for the Barnett and Marcellus Shales; their study demonstrated the significance of geomechanics in production analysis, especially for reservoirs with low Young's modulus. McClure (2014) conducted a series numerical simulation studies to model the geomechanics effect on water-loss mechanisms during flow-back; they concluded that water recovery was reduced due to fracture closure and trapping of fluid away from the main hydraulic fracture. However, the model was based on single-phase flow. Chu et al. (2015) incorporated in their simulation models the additional effects of critical gas saturation enhancement and bubble-point pressure suppression due to compaction of nano-pores in shale matrix; however, secondary fractures were not explicitly represented in their models.

There are four major deficiencies in these previous numerical studies regrading geomechanics: (1) the coupling of stress-dependent fracture conductivity and multiphase flow functions in both fracture and matrix systems is incomplete. Water and oil re-distribute due to counter-current imbibition upon shut-in, and fluid pressure inside the fracture system drops; hence, fracture compacts and further influence the imbibition process; (2) although Sherman et al. (1991) and Osholake et al. (2013) have investigated the impacts of operational conditions on water loss and production, detailed understanding of the sensitivity of stress-dependent fracture conductivity relationships coupled with different operational conditions is still lacking; (3) the combined impact of solution gas and fracture compaction during flow-back is less understood; and (4)

previous studies assumed symmetrical and fully-connected secondary fracture networks, which fail to capture the realistic heterogeneous fracture distribution commonly observed in unconventional reservoirs and the non-uniform connection between secondary fractures and the main hydraulic fracture. The effect of disconnected secondary fracture network on water recovery and oil production has only been alluded to in the past. Therefore, stochastic discrete fracture networks are adopted in this study to capture the complexity and heterogeneity of the fracture systems.

Chapter 3: Methodology

A commercial black oil simulator is used to construct a series of 2-D mechanistic model (CMG IMAX, 2013). Three systems: hydraulic fracture (HF), secondary fractures (NF), and matrix (M), are modeled explicitly following the single-porosity approach by assigning higher porosity and permeability in the fracture cells and lower porosity and permeability in the matrix cells (**Fig. 3.1**). There is no restriction of flow direction and the number of fluid phases in the model, and flow in fracture-fracture, matrix-fracture and matrix-matrix connections are simulated in detail (Karimi-Fard *et al*., 2004; Qasem *et al*., 2008; Rubin 2010). Hydraulic fracture stages are assumed to be evenly spaced and symmetrical. A top view of a segment of a horizontal well along x-direction with a bi-wing hydraulic fracture is shown in **Fig. 3.1**. Perforation position is the intersection of hydraulic fracture and horizontal well.

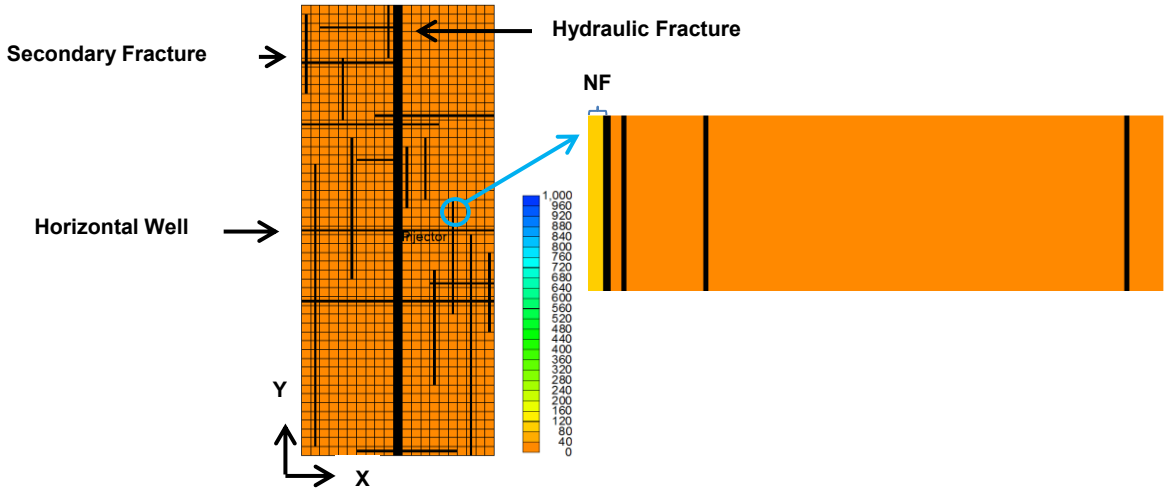

Fig. 3. 1 Top view of fracture and permeability distribution for the base case

3.1 Mechanistic Model Description

A set of 2-D 210 m × 510 m models is constructed. Relevant reservoir, fluid, and well parameters for base case are summarized in **Table 3.1**. According to CMG IMEX (2013), fractures with the same conductivity, $k_F \times a_F$, but different specific combinations of k_F and a_F, would result in the same flow performance. Therefore, in order to avoid numerical instability due to large disparity in permeability values among the fracture and matrix cells, the fracture cell width and its corresponding permeability are assigned in accordance to the fracture conductivity for a particular set of k_F and a_F values as shown in **Table 3.1**. Parameters used in this simulation study are modified from that representative of the Bakken tight oil reservoirs, as presented in Yue *et al*. (2013). The range of secondary-fracture permeability used in this study is 3mD – 100mD (Rubin, 2010; Cheng 2012; Fakcharoenphol *et al*., 2013; Yue *et al*., 2013; Wattenbarger *et al*., 2013). The range of matrix permeability used in this study is 0.0005mD – 0.0025mD. The PVT data and multiphase flow functions for the water-oil and liquid-gas systems are presented in **Fig. 3.2**, **Fig. 3.3** and **Fig. 3.4**. Distinct two-phase relative permeability functions for the water-oil and liquid-gas systems are assigned to the three porosity systems (HF, NF, M). Stone's second model (Stone 1973) is used to evaluate the three phase oil relative permeability. Relative permeability functions for oil-water two-phase flow in water-wet formation are assigned to three porosity systems (HF, NF, M) according to Kazemi *et al*. (1976) and Aguilera (1980). Negligible capillary pressure is assigned in HF due to its high conductivity. On the other hand, separate capillary pressure functions are employed for the matrix and secondary fracture systems respectively according to Kazemi *et al*. (1976) and Aguilera (1980). Capillary pressure functions for matrix and secondary fracture systems are assigned according to the correlation in Eq. (3.1), which is adopted from Gdanski *et al*. (2009) and a variation of the "Leverett j-function"

(Leverett 1941).

$$P_c = \frac{\sigma'}{a_2 (S_w)^{a_1}} \left(\frac{\phi}{k}\right)^{a_3} \times 6894.76 \quad \text{.....(3.1)}$$

Interfacial tension of water and oil (σ′) is 30 dynes/cm for the water-oil system and 4 dynes/cm for the liquid-gas system; For the matrix, a_1 = 1.86 and a_2 = 6.42, representative of low-permeability rocks described in Holditch (1979); a_3 (a measure of pore structure) = 0.5 (Bradley 1992). Assuming that the same Leverett j-function can describe the $P_c - S_w$ functions in both the matrix and the secondary fracture, the $P_c - S_w$ function corresponding to the secondary fracture is computed by scaling the Leverett j-function with values of ϕ_{NF} and k_{NF}; the constants a_1, a_2 and a_3 are obtained as fitting parameters via regression of Eq. 1.Therefore, for the secondary fractures, a_1 = 0.79, a_2 = 0.32 and a_3 = 0.5. Examples of capillary pressure functions for different permeabilities in M and NF are shown in **Fig. 3.5**. Initial water saturation in hydraulic fracture and induced secondary fracture are higher than that in matrix. A short water injection period is followed by a shut-in period to model leak-off of fracturing fluid and a realistic fracturing fluid efficiency less than 100% (Zanganeh et al. 2014). Water and oil re-distribute due to viscous and capillary forces during this shut-in. Upon re-opening the well, the fracturing fluid is flown back with produced oil. This mechanistic model simulates this shut-in and subsequent flow-back or production periods. Simulation boundary conditions including well constraints are presented in **Table 3.1**. The total water injection volume for base case is 54m^3 (which is the initial volume of water in the HF and the NFs that are connected to the HF, plus the water volume injected at a rate of 90m^3/day over a duration of 0.5 hour).

Table 3. 1 – Reservoir, well and fluid properties for the base case

Parameters	Value
Initial reservoir pressure P_i	4.69×10^{7} Pa
Minimum wellbore flowing pressure P_{wf}	3.50×10^{7} Pa
Total compressibility C_t	2.51×10^{-9} Pa^{-1}
Bubble point pressure P_b	3.50×10^{7} Pa
Matrix permeability k_M	0.5×10^{-18} m^2
Secondary fracture (NF) conductivity $k_{NF}\cdot a_{NF}$	5×10^{-16} m^3
Hydraulic-fracture (HF) conductivity $k_{HF}\cdot a_{HF}$	2×10^{-14} m^3
Matrix porosity ϕ_M	0.09
Secondary fracture porosity ϕ_{NF}	0.6
Hydraulic-fracture porosity ϕ_{HF}	0.8
Matrix initial water saturation S_{wM}	0.2
Secondary fracture initial water saturation S_{wNF}	1 (Connected with HF)
Secondary fracture initial water saturation S_{wNF}	0.05 (Not connected with HF)
Hydraulic-fracture initial water saturation S_{wHF}	1
Surface water injection rate q_{winj}	90 m^3/day
Water injection duration t_{winj}	0.5 hr

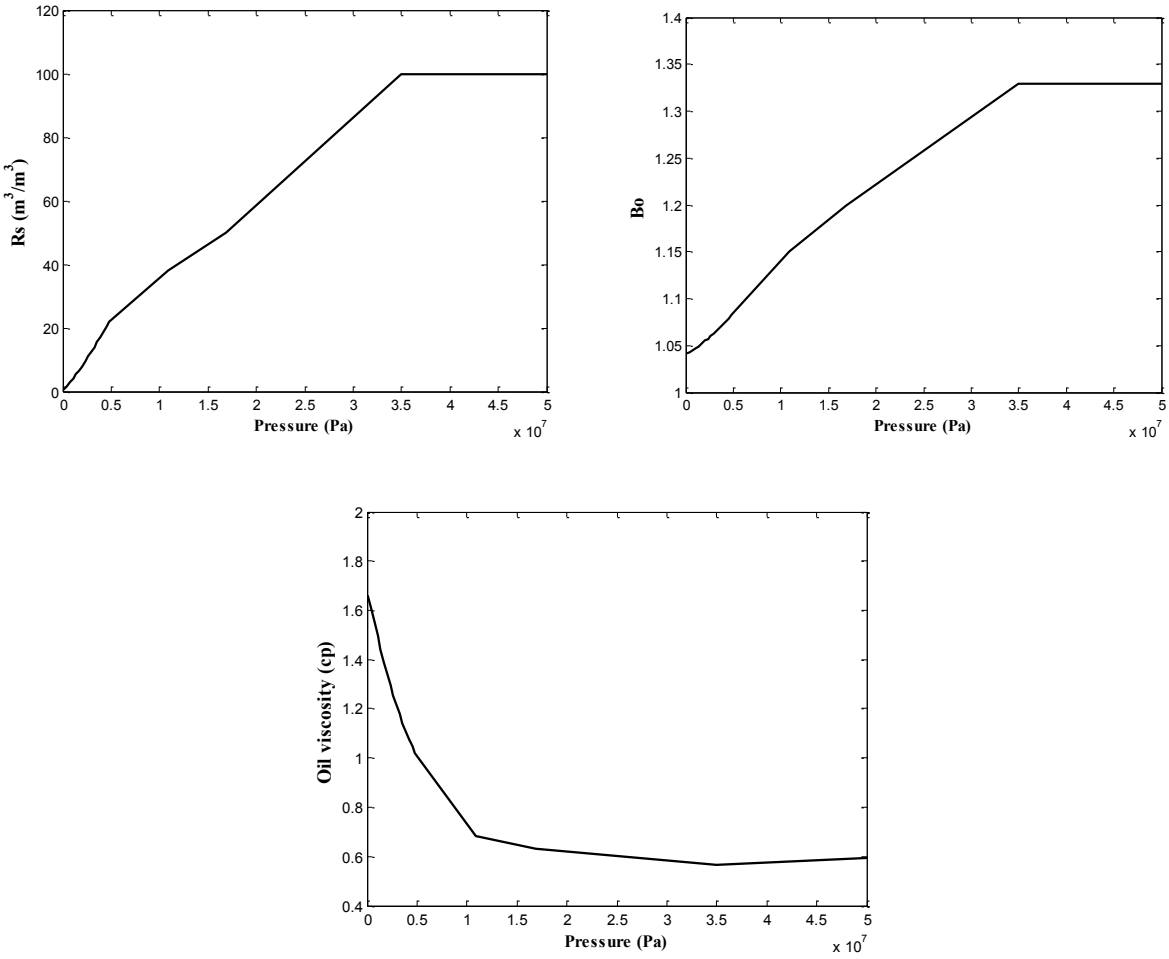

Fig. 3. 2 PVT properties of the reservoir fluid

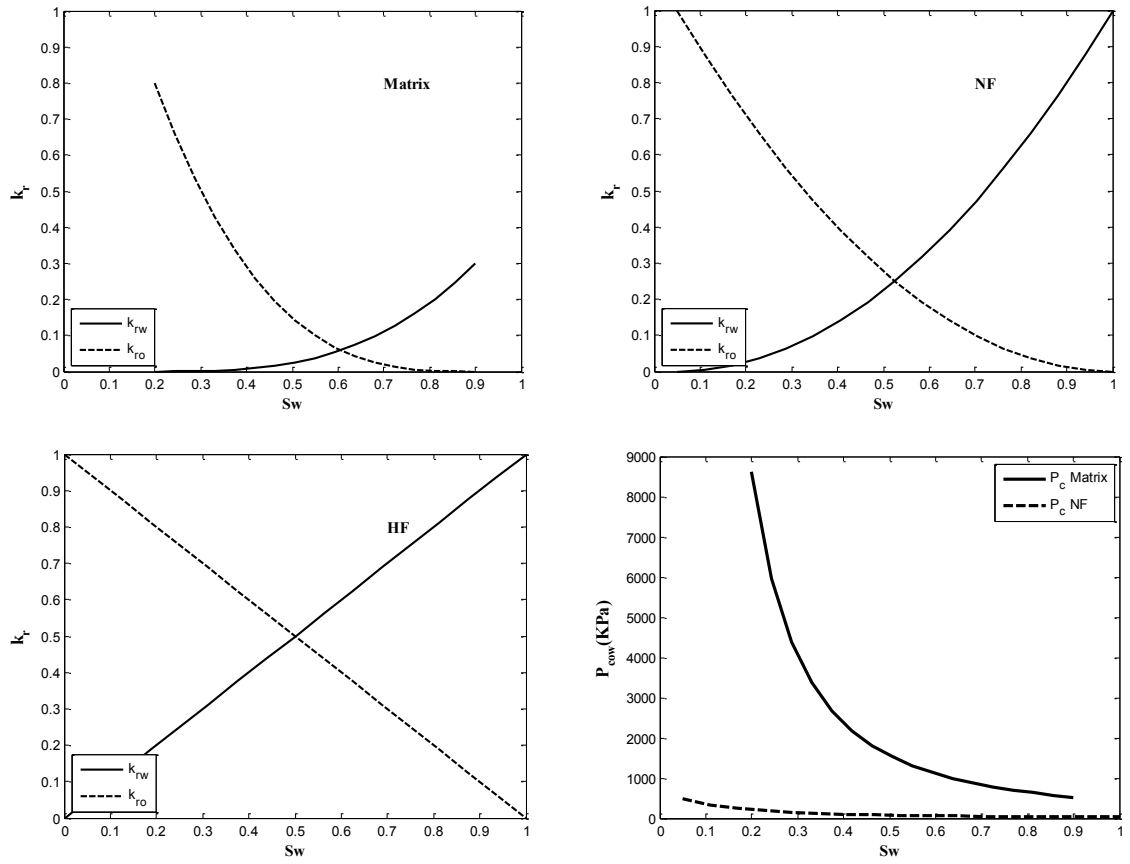

Fig. 3. 3 Water-oil relative permeability and capillary pressure functions for matrix and fractures in the base case

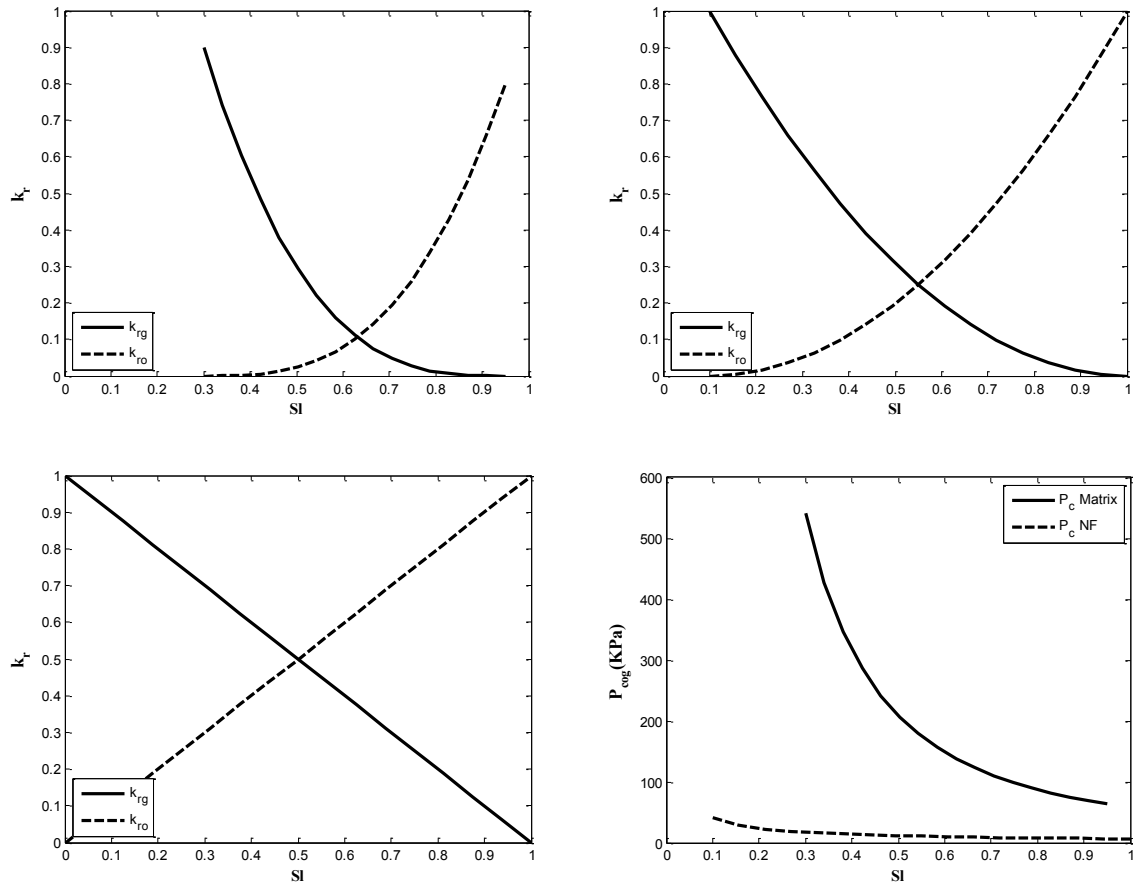

Fig. 3. 4 Liquid-gas relative permeability and capillary pressure functions for matrix and fractures in the base case

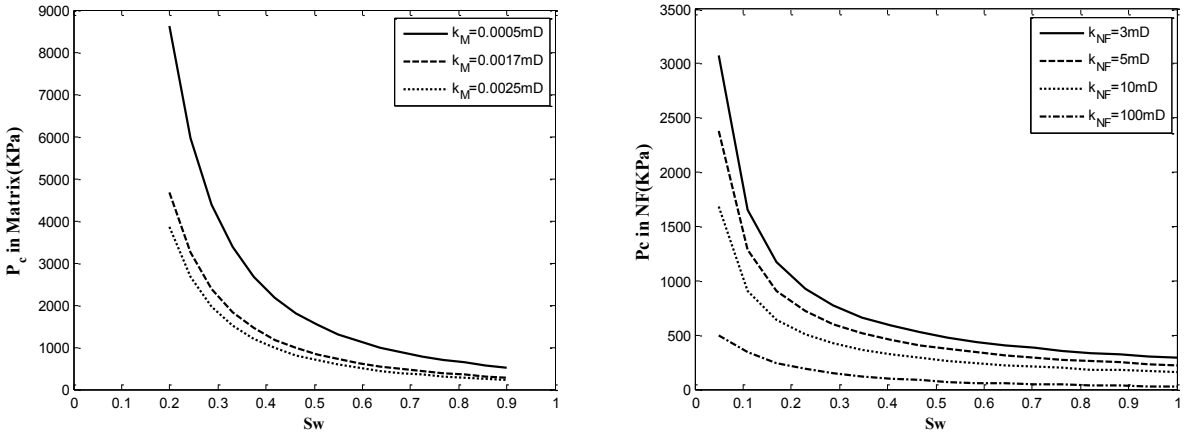

Fig. 3. 5 Capillary pressure as a function of matrix and secondary-fracture permeability

3.2 Discrete Fracture Network Model

Typically only a fraction of the fracture network in the domain can be observed near wellbore, a deterministic modeling of the entire fracture network is impossible (Chilès 2005). Many approaches have been developed to generate stochastic fracture network models via Monte Carlo sampling; these methods include the Poisson model, Truncated Poisson model, Parent-Daughter model, Hierarchical model, Fractal model, and multiple-point statistics (Chilès 2005; Clemo 1994; Eskandari *et al*., 2010). In these models, fracture parameters are sampled stochastically from a set of probability distributions. Depending on the complexity of the problem, these parameters could be correlated and described by a multivariate distribution. In addition, conditioning of geologic and well observations can be integrated (Sil *et al*., 2009). As discussed in Chapter 2, stochastic fracture networks can capture the uncertainty of fracture parameters and their influences multiphase flow behavior.

It is assumed that the location and orientation of each fracture are independent from other fractures. Fractures centers are distributed randomly in the domain with a constant expected density. The relevant steps are outlined.

(1) Total number of secondary fractures in the domain, N_f, is sampled from the Poisson distribution for a univariate random variable (Stoyan *et al*., 1994), as described by Eq. (3.2) and Eq. (3.3).

$$P(X = x) = \begin{cases} \dfrac{e^{-\mu}\mu^{x}}{x!} & x \geq 0 \\ 0 \quad otherwise \end{cases} \qquad (3.2)$$

$$P(X \leq x) = \begin{cases} Q([x]+1, \mu) & x \geq 0 \\ 0 \quad otherwise \end{cases} \qquad (3.3)$$

Where Q[x] is regularized incomplete gamma function and μ is the mean;

(2) Centers (midpoints) of N_f fractures are sampled independently from a binomial distribution (Stoyan *et al*., 1994).

(3) Lengths of N_f fractures are sampled from a log-normal distribution (Clemo 1994), as described by Eq. (3.4) and Eq. (3.5).

$$P(X=x)=\begin{cases}\dfrac{e^{-\frac{(\log(x)-\mu)^2}{2\sigma^2}}}{\sqrt{2\pi}\sigma x} & x>0\\ 0 \quad otherwise\end{cases} \qquad (3.4)$$

$$P(X\le x)=\begin{cases}\dfrac{1}{2}erfc(\dfrac{\mu-\log(x)}{\sqrt{2}\sigma}) & x>0\\ 0 \quad otherwise\end{cases} \qquad (3.5)$$

Where σ is the standard deviation;

(4) Orientation of N_f fractures are assigned for two sets of secondary fractures, assuming equal probability of orientation along x- or y- axis;

(5) Multiple realizations are constructed with the Monte Carlo sampling procedure in steps (1) - (4). Each realization is subjected to numerical simulation to model fluid flow during shut-in and flow-back. Six randomly-selected realizations are shown in **Fig. 3.6**.

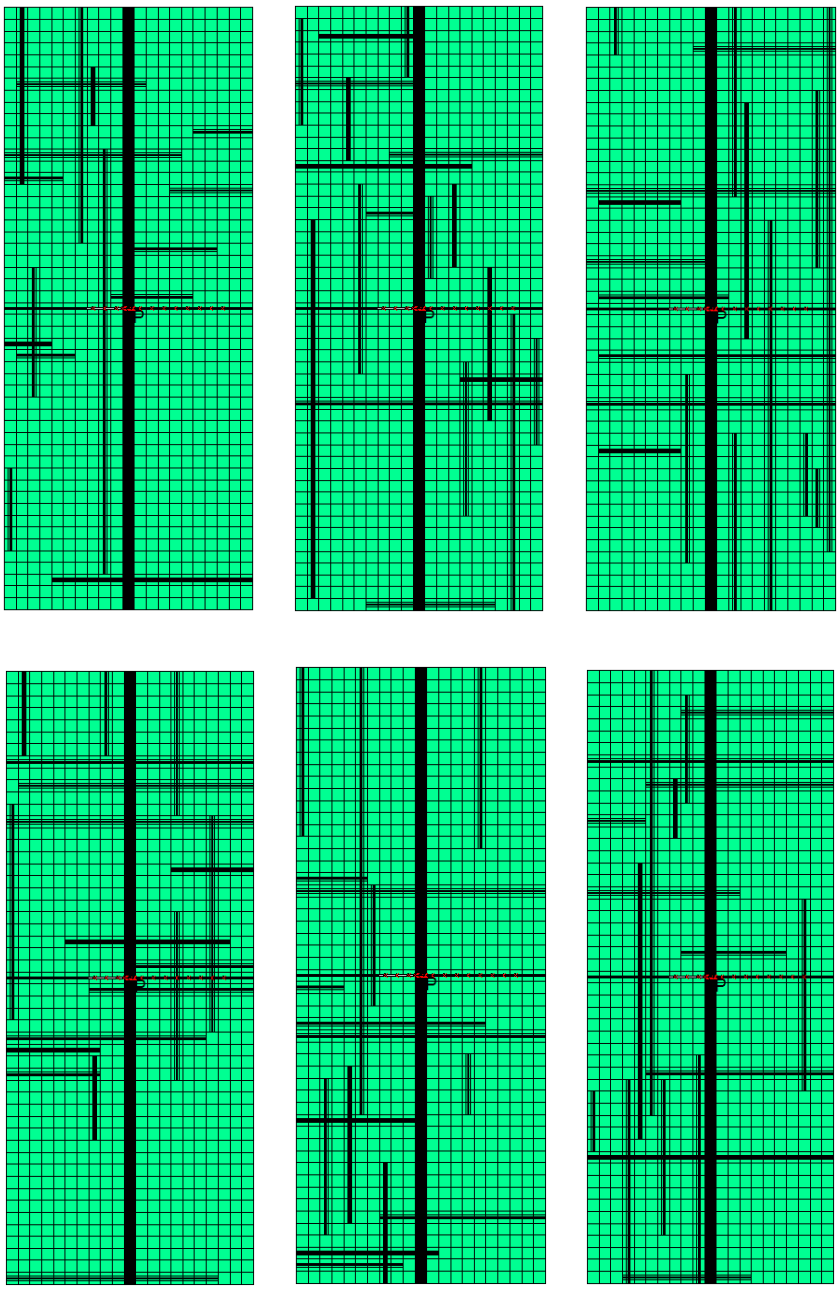

Fig. 3. 6 Examples of different DFN realizations. The red dot in the center indicates the perforation point.

Fracture intensity – P_{32}, defined by Eq. (3.6) – and volume of secondary fractures connected to the hydraulic fracture are calculated for each realization. Each realization is subjected to numerical multiphase flow simulation to model fluid movement and distribution during shut-in

and flow-back.

$$P_{32} = \frac{Area\ of\ NF}{Bulk\ volume} \quad \text{..... (3.6)}$$

3.3 Local Grid Refinement

Due to the vastly different dimensions of fracture grid and matrix cells, logarithmic local grid refinement (Eq. 3.7) is used for discretizing regions around the fractures to enhance the consistency and stability of the numerical solution.

$$w = \frac{a_F}{2}\exp[\frac{2n}{N-1}\ln(\frac{2w_e}{a_F})] \qquad (n = 0,1,2,....) \quad \text{..... (3.7)}$$

Where a_F is fracture aperture, n is the index of individual refined grid – no larger than $(N-1)/2$, N is the total number of refined grids, w_e is half width of the parent grid, and w is the distance from a particular refined grid outer boundary to the center of parent grid, where the fracture is located. The above equation allows the width of each refined grid to be calculated.

Local grid refinement (LGR) is particularly important in areas with large pressure and saturation gradient. Abrupt changes and discontinuities compromise the consistency and stability of the numerical solution. A total of 15 refined grids in a parent grid are used in this study, providing a reasonable balance between the quality of numerical solution and computational efficiency.

3.4 Modeling of Stress-Dependent Fracture Conductivity

For the hydraulic fracture, Alramahi *et al*. (2012) and Yu *et al*. (2014) developed the following relationship between normalized fracture conductivity (with respect to the fracture conductivity

measured at 3.45×10^6 Pa) and closure stress from experimental measurement conducted using high-strength proppant bauxite:

$$\log(F_{cd}) = \begin{cases} -1.5\times10^{-7}\times\sigma_c - 15.63 & \textit{Stiff Formation} - 3.45\times10^{10} < E < 6.89\times10^{10}\ Pa \\ -5.8\times10^{-7}\times\sigma_c - 15.30 & \textit{Medium Formation} - 1.38\times10^{10} < E < 3.45\times10^{10}\ Pa \\ -8.7\times10^{-7}\times\sigma_c - 15.95 & \textit{Soft Formation} - E < 1.38\times10^{10}\ Pa \end{cases} \quad (3.8)$$

F_{cd} is the normalized fracture conductivity (m^2-m), σ_c is the closure stress (Pa) for hydraulic fracture and E is the Young's Modulus.

For the secondary fracture, Cho *et al*. (2013) verified through lab experiments the exponential relationship between permeability and pressure change (Eq. 3.9), which was initially proposed by Raghavan *et al*. (2002) for non-fractured rocks.

$$k = k_0 e^{-b\sigma'} \quad (3.9)$$

The parameter k_0 refers to the permeability when the effective mean stress (σ′) equals to zero, and b is an empirical constant determined experimentally. According to Eq. 3.9, it can be deduced that the logarithm of normalized fracture conductivity should follow a linear relationship with the closure stress. Therefore, a set of equations, similar to those in Eq. 3.8, are developed from Cho *et al*. (2013) for the secondary fracture:

$$\ln(F'_{cd}) = \begin{cases} -0.0004\times\sigma'_c & \text{Stiff Formation} \\ -0.0011\times\sigma'_c & \text{Medium Formation} \\ -0.0016\times\sigma'_c & \text{Soft Formation} \end{cases} \quad (3.10)$$

F'_{cd} is the normalized fracture conductivity (m^2-m) and σ'_c is the closure stress (Pa) for secondary fracture. Minimum and maximum horizontal stresses of 7.33×10^7 Pa and 8.01×10^7 Pa are assumed to calculate closure stress. Hydraulic fracture is placed perpendicular to the minimum horizontal stress, while secondary fractures are oriented either parallel or

perpendicular to the hydraulic fracture. Initial fracture conductivities are computed using Eq. 3.8 and Eq. 3.10, and the value of σ_c depends on the fluid pressure inside the fracture (e.g., a value of 2.64×10^7 Pa corresponds to an initial reservoir pressure of 4.69×10^7 Pa). To model the stress-dependent fracture conductivity with pressure decline, correlations derived from experimental data in Alramahi *et al*. (2012) and Cho *et al*. (2013) of fracture conductivity multiplier (fracture conductivity at a certain closure stress normalized against that measured at initial closure stress), as illustrated in **Fig. 3.7**, are adopted. Following the suggestion by Rubin (2010), change in fracture conductivity is realized by modifying fracture permeability while keeping fracture width and porosity constant.

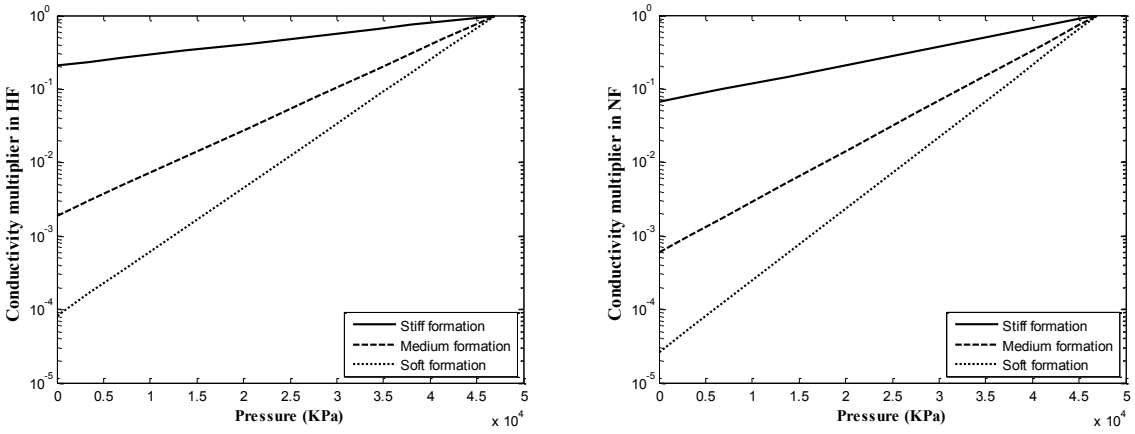

Fig. 3. 7 Fracture conductivity multiplier as a function of fluid pressure inside the fracture

Chapter 4: Water Retention in Matrix and Secondary Fractures

First, the numerical simulation is validated against field observations using a randomly-selected case, where N_f and secondary fracture length follows the Poisson distribution (μ = 20) and log-normal distribution (μ = 1.8m, σ = 0.6m), respectively (**Fig. 4.1**). **Fig. 4.2** presents the corresponding production profiles after shut-in duration of 23.5 hours. The production trends are in good agreement qualitatively with those observed in the field, as by Abbasi *et al*. (2014) and shown in **Fig. 4.3**. **Fig. 4.2-4.3** show that oil production is negligible at the beginning of flow-back, while water rate continues to decrease during the production phase. For the simulation case, oil production is zero when flow-back commences, and it continues to rise after approximately 25 hours; the initial high water rate, on the other hand, continues to decline as flow-back progresses. A total fracturing fluid recovery of 50% is predicted using the numerical model, which is consistent with field measurement.

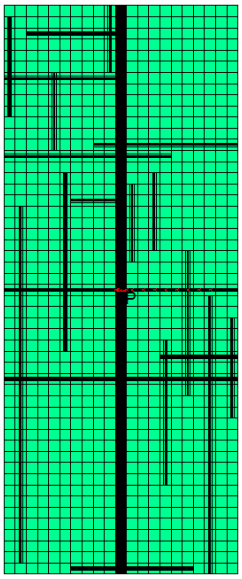

Fig. 4. 1 Schematic of fracture distribution in the base case

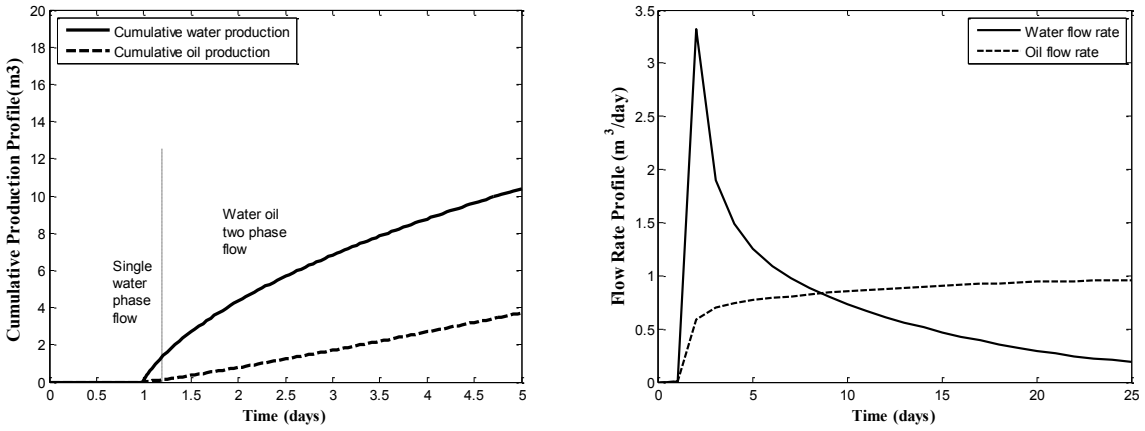

Fig. 4. 2 Typical oil and water production profiles from numerical simulations

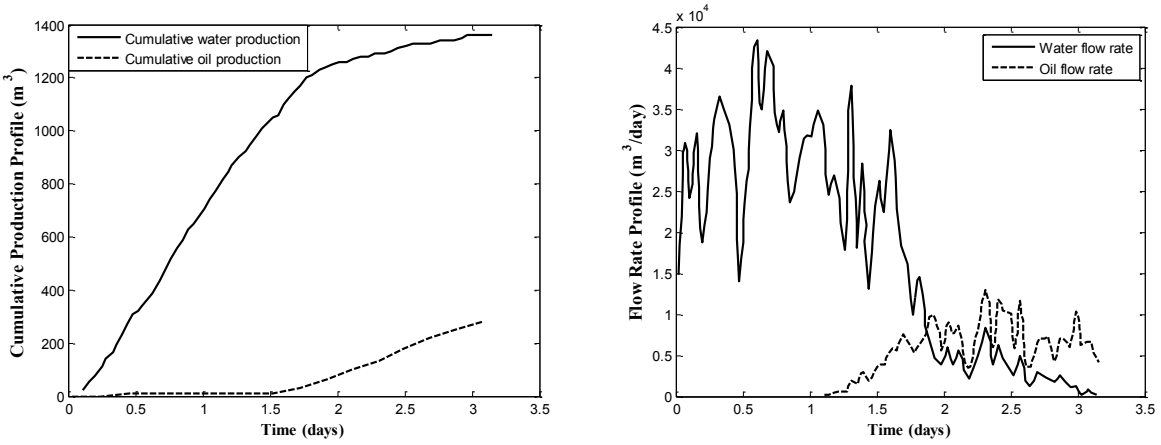

Fig. 4. 3 Field oil and water production data adapted from Abbasi et al. (2014)

Although a quantitative match with actual flow-back data would be ideal, this type of match is difficult to achieve. Daily production data are generally recorded, but other important data such as high-frequency flow-back rates, reliable bottom-hole pressure measurements during shut-in and detailed characterization of fracture systems, are not readily available, rendering it extremely

challenging to validate the simulation results quantitatively. This difficulty has led to some confusion among practitioners about the origins and impacts of water loss. Therefore, various numerical experiments are conducted in this study to explore how water loss could be influenced by various factors.

Next, in order to interpret the results of the subsequent sensitivity analysis, a base case is constructed using the previous NF configuration (**Fig. 4.1**) with a shut-in duration of 16 weeks. The water saturation distribution at the end of the injection period is presented in **Fig. 4.4**.

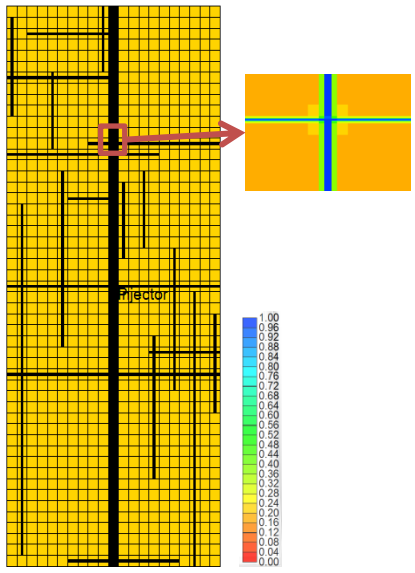

Fig. 4. 4 Water saturation distribution at the end of the injection period

Water-phase pressure profiles and saturation changes in the fracture and matrix systems during shut-in are shown in **Fig. 4.5**. Water saturation in matrix surrounding the fractures increases with time. Upon shut-in, pressure differential across fracture and matrix interface is high, causing viscous force to dominate. As the pressure differential declines, capillary force becomes more

important; this would also explain the slight increase in fracture pressure near the end of shut-in, according to the pressure equation (Eq. 4.1) commonly implemented in finite-difference simulators (Ertekin et al., 2001). A total water recovery of 25% can be observed from the oil and water production profiles as shown in **Fig. 4.6**. According to the water saturation equation (Eq. 4.2) in finite-difference simulators (Ertekin et al., 2001), decrease in fracture water saturation as a result of imbibition can occur as long as the fracture water-phase pressure is higher than that in the matrix, regardless of whether it is higher or lower than the non-wetting-phase pressure in the surrounding matrix. For example, as evidenced in **Fig. 4.5**, the water-phase pressure in fracture is approximately 6000KPa higher than the oil-phase pressure in the surrounding matrix after 0.5 hour of shut-in; while after 100 days, water-phase pressure in fracture has dropped below the oil-phase pressure in the surrounding matrix. In both cases, imbibition has continued.

$$c_{tF}V_{pF}\frac{\Delta P_F}{\Delta t} = -\lambda_{rt}(T)_{F-M}\left(P_F - P_M\right) - B_o\lambda_{ro}(T)_{F-M}\left(Pc_F - Pc_M\right) \quad \text{.....(4.1)}$$

$$\Delta S_{wF} = -\frac{\Delta t}{V_{pF}}\left(B_{wF}\lambda_{rw}\right)(T)_{F-M}\left(P_F - P_M\right) \quad \text{.....(4.2)}$$

where c_t is total compressibility, V_p is pore volume, P is water-phase pressure, Δt is the duration of one time step, λ_{rt} is total relative mobility, λ_r is relative mobility, $T_{F\text{-}M}$ is transmissibility between the matrix and fracture cells, B is formation volume factor, P_c is capillary pressure, S_w is water saturation. Subscripts F and M denote fracture and matrix, respectively. Subscripts w and o refer to water-phase and oil-phase properties, respectively.

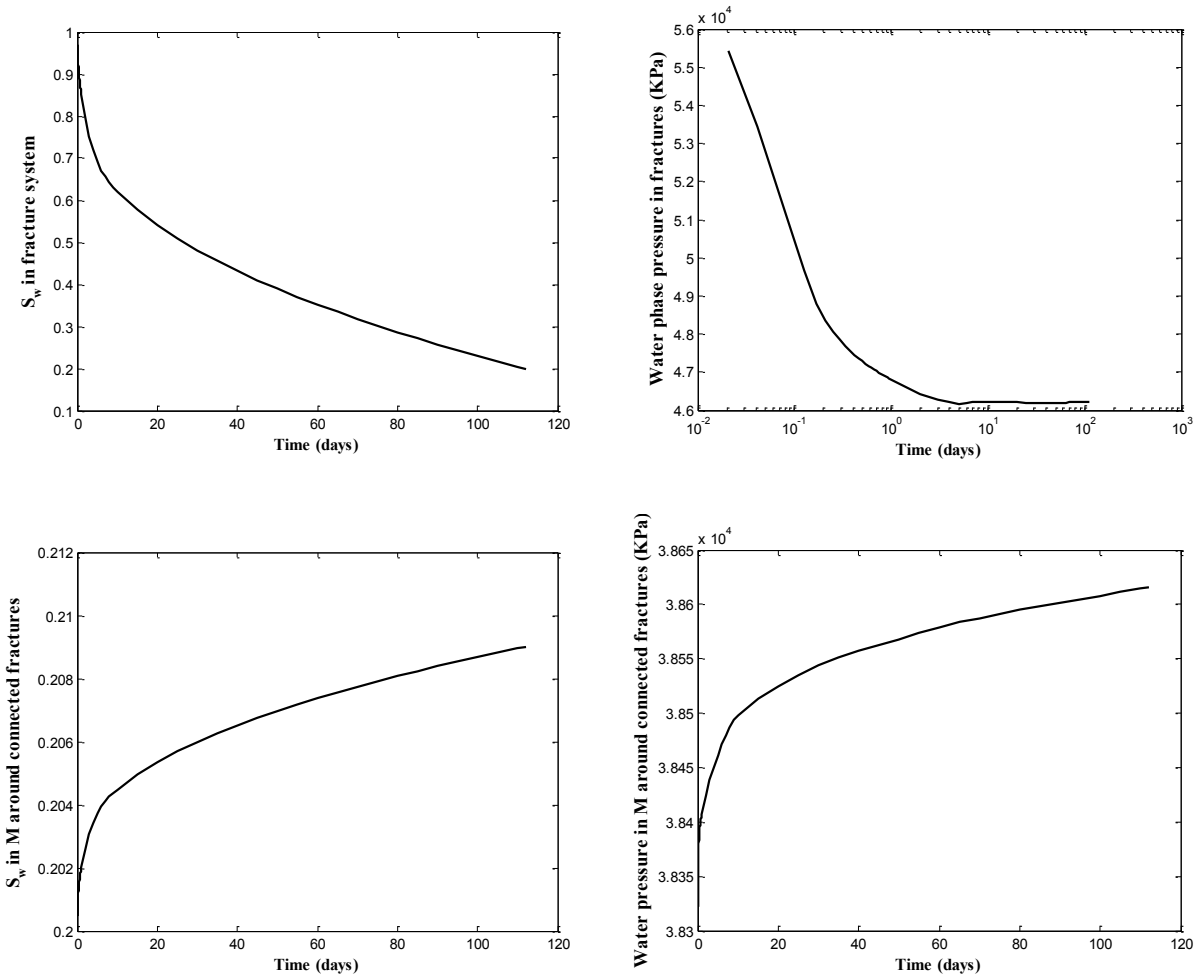

Fig. 4. 5 Water-phase pressure and saturation profiles during shut-in for the base case

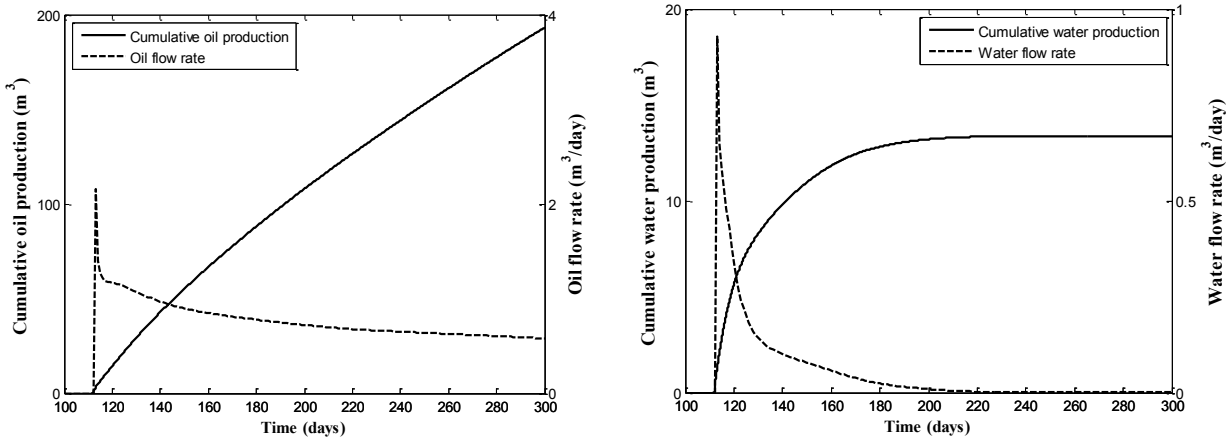

Fig. 4. 6 Water and oil production profiles for the base case

4.1 Water Loss in Matrix

Given high capillary pressure in tight rocks, countercurrent imbibition is a dominant drive mechanism, and this process is influenced by matrix permeability and capillary pressure, secondary fracture properties (size, intensity, and connectivity), shut-in duration and initial matrix water saturation (desiccated scenario).

4.1.1 Impacts of Secondary Fracture Properties and Shut-in Duration

A series of DFN model is generated in this study. Two Poisson distributions (μ = 20 and 30) are used for fracture intensity and three log-normal distributions μ = 1.2m, 1.5m and 1.8m) are used for fracture length. Five realizations are generated for each combination of N_f and fracture-length distributions (a set of 3 × 2 = 6 combinations can be obtained.) Therefore, a total of 30 realizations, encompassing a large range of fracture intensity and connectivity for sensitivity analysis, are constructed. Variability between individual realizations could lead to slight variation (< 5%) in initial water content in secondary fracture.

First, a series of models with different secondary fracture length distributions is employed to investigate its impact on matrix imbibition and flow-back performance. Considering the two extreme scenarios from **Fig. 4.7**, where two realizations consisting of short fractures are sampled from a lognormal distribution of μ = 1.2 and σ = 0.6, while another two realizations of long fractures are sampled from a lognormal distribution of μ = 1.8 and σ = 0.6. It can be observed from **Fig. 4.7** that water has imbibed into matrix in the regions around the secondary fractures at the end of shut-in. Increase in fracture length creates a larger fracture-matrix contact area and promotes more matrix imbibition; as a result, water production during flow-back is reduced, as

illustrated in **Table 4.1**, in which the production averaged over 5 cases with the same fracture length distribution are shown. There is an approximately 10% difference in cumulative water production at the end of 300 days. Relative permeability to oil phase in the fractures is higher at reduced water saturation, hence the cumulative oil production has also increased and there is a 45% difference of cumulative oil production at the end of 300 days. Water imbibition into the matrix from the secondary fractures is higher than that from the hydraulic fractures. The possible reasons are 1) more water is leaking off into the surrounding matrix from the hydraulic fracture during injection; thus, higher water saturation near the hydraulic fracture upon shut-in would lead to slower imbibition in regions close to the hydraulic fracture; and 2) at the end of injection period, fluid pressure in the hydraulic fracture is higher than that in the secondary fracture; as will be discussed in section 4.2.2, higher fluid pressure in fracture would result in lower imbibition rate.

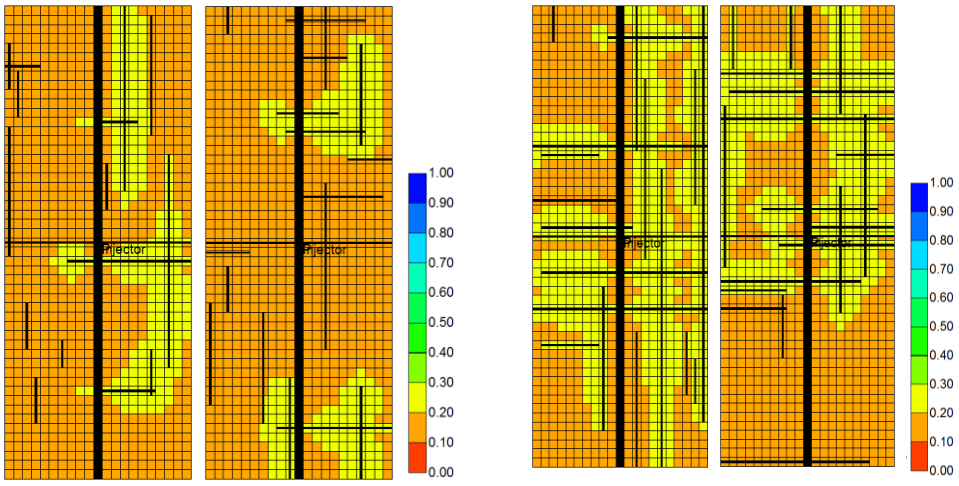

Fig. 4. 7 Water saturation at the end of shut-in for lognormal fracture length distribution of μ = 1.2, σ = 0.6 (left) and μ = 1.8 and σ = 0.6 (right)

Table 4. 1 Average oil and water recovery at 300 days for different NF length distribution

Length distribution	Cumulative oil production (m^3)	Cumulative water production (m^3)
Lognormal (1.2,0.6)	176.30	14.06
Lognormal (1.8,0.6)	253.84	12.77

Second, the relationships between production performance and connected fracture volume are investigated. For each of the 30 fracture network realizations, volume of secondary fractures connected to the hydraulic fracture is calculated. This connected network encompasses secondary fractures that are directly intersecting the two bi-wings of the hydraulic fracture and additional secondary fractures that are indirectly connected. Cross-plots between IP30 (initial oil production over 30 days), long-term cumulative oil production over 300 days, water recovery after 300 days and the connected secondary fracture volume are shown in **Fig. 4.8**. In addition to the increased fracture-matrix interface area for counter-current imbibition to occur, increased connected volume also implies that there is increased water content surrounding the matrix upon shut-in. Redistribution of water and oil during imbibition results in a higher oil content within a larger connected volume and improves oil production. Uncertainty in secondary fracture network connectivity leads to 35.43% variation in water recovery after 300 days, and 120% variation in 300-day cumulative oil production. The volume of connected fracture volume is also directly related to the simulated reservoir volume (SRV). Due to the low matrix permeability, hydrocarbons depletion in regions located far away from the connected fracture system is minimal. These results confirm the notion that given similar matrix properties and operational conditions (such as shut-in duration), water recovery volume during flow-back can be correlated

to SRV. Since fracture intensity P_{32} is positively correlated with connected fracture volume, as shown in **Fig. 4.8**, either P_{32} or connected fracture volume can be used to explain the positive short-term and long-term impacts of enhanced matrix imbibition due to enlarged contact area between fracture and matrix.

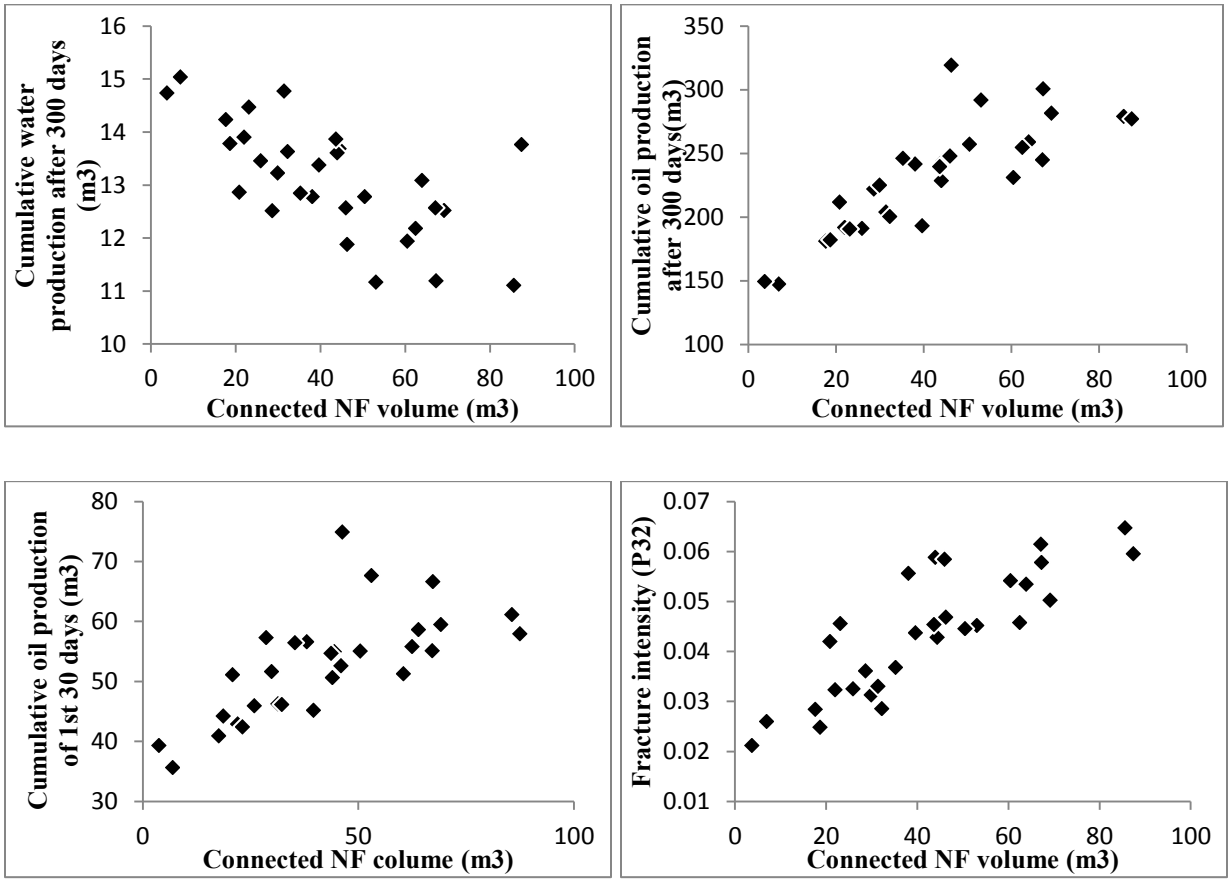

Fig. 4. 8 Cross-plots between IP30, cumulative water production, cumulative oil production and fracture intensity (P_{32}) against connected volume

It is important to note that water imbibition into the matrix is often a slow and transient process. As shut-in progresses, water would slowly imbibe deeper into the matrix formations until steady-state is reached and water saturation S_{wM} rises to a constant level. However, the typical shut-in period is often less than a few weeks; much of the water in the fractures would flow back to the

hydraulic fracture when production resumes. In addition, except under certain special conditions (e.g., matrix being initially desiccated or existence of a saturation range over which there is no multiphase flow), water cannot be trapped in the matrix indefinitely. In reality, its flow rate is very slow that it appears to be immobile within the matrix. Therefore, the time scales associated with matrix imbibition is investigated. Base case with connected NF volume of 40 m^3 is subjected to a number of operational scenarios with 3 different shut-in durations: 2 weeks, 8 weeks and 16 weeks. Water saturation distributions at the end of different shut-in durations are shown in **Fig. 4.9**. Oil and water production profiles are shown in **Fig. 4.10**. A few observations can be drawn: 1) as shut-in time increase, imbibed water penetrates deeper into matrix; as a result, water loss increases and flow-back volume decreases; 2) due to counter-current imbibition, more oil would drain into the fracture network after a prolonged shut-in; high conductivity in the fractures helps to increase the initial oil flow rate; 3) the increase in oil rate appears to be for the short term; no observable long-term improvement in production can be detected from extended shut-in. Same result is also presented in Cheng (2012). Some possible explanation are that 1) the imbibition is slow and would affect only a limited region surrounding the water-filled connected fracture networks; 2) even though extended shut-in duration can cause higher water saturation in the matrix around fracture and lower oil relative permeability during flow back period due to capillary-end effect, water saturation in the HF is lower due to extended shut-in duration, which can cause higher oil relative permeability in the fracture and mitigate the adverse effect caused by capillary-end effect (**Table 4.2**). Therefore, the impacts of extended shut-in duration are limited to short-term performance. It should also be emphasized that this observation appears to be valid with matrix imbibition being the only water-loss mechanism. If additional water-loss mechanisms such as secondary fracture trapping and closure of induced

fractures are included, impacts on long-term production might be more pronounced.

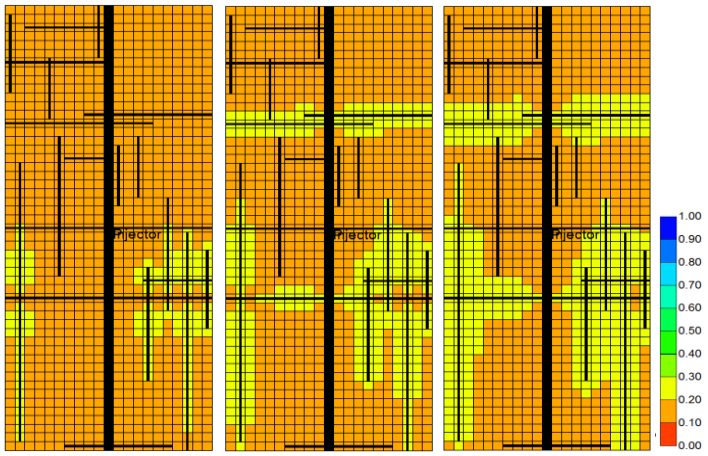

Fig. 4. 9. Water saturation distribution after shut-in of 2 weeks, 8 weeks and 16 weeks, respectively

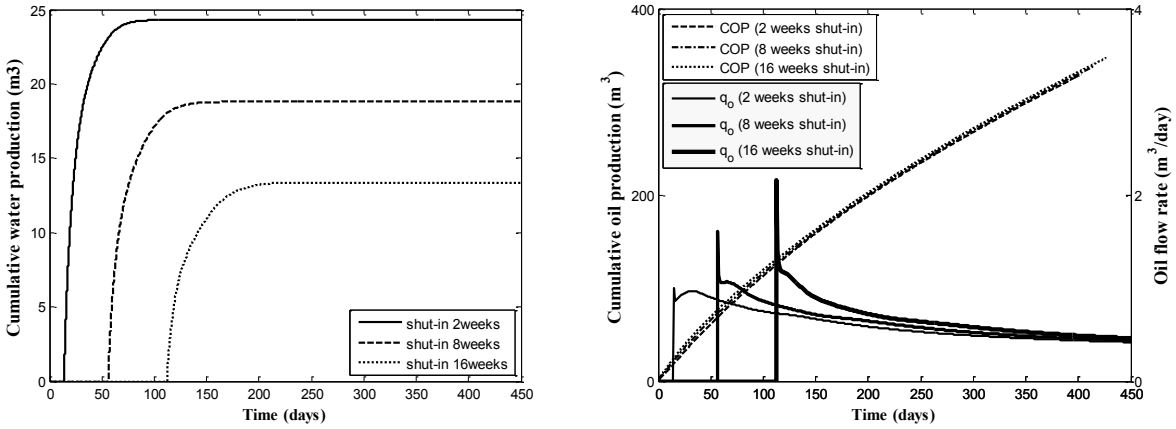

Fig. 4. 10 Cumulative water production, initial oil flow rate and cumulative oil production (from the end of soaking period) profiles

Table 4. 2 Water saturation distribution at the beginning of flow-back

Shut-in Duration	Distance from HF surface (m)				
	HF	0.0075	0.03	0.06	0.1025
2 weeks	0.6859	0.7391	0.5751	0.445	0.2884
8 weeks	0.4487	0.7717	0.6353	0.5463	0.4484
16 weeks	0.2538	0.7898	0.663	0.5865	0.5083

From above analysis, both secondary fractures and shut-in duration can influence flow-back water quantity and short-term oil production; however, only secondary fractures can enhance matrix-fracture contact area and improve long-term oil production. This observation can be further illustrated by comparing case (A) with P_{32} of 0.0361 and secondary fracture connectivity of 28.645m^3 with another case (B) with P_{32} of 0.065 and connectivity of 3.295m^3. It can be shown that same quantity of flow-back water is recovered after 112 days and 97 days for cases (A) and (B), respectively. The subsequent oil production profiles for both cases are shown in **Fig. 4.11**. Although short-term oil production is the similar, only long-term oil production is higher for case with higher secondary fracture intensity and connectivity. An important conclusion is that high initial rate can be a result of prolonged shut-in, while actual long-term enhancement in production can only be attributed to extensive connected secondary fracture networks.

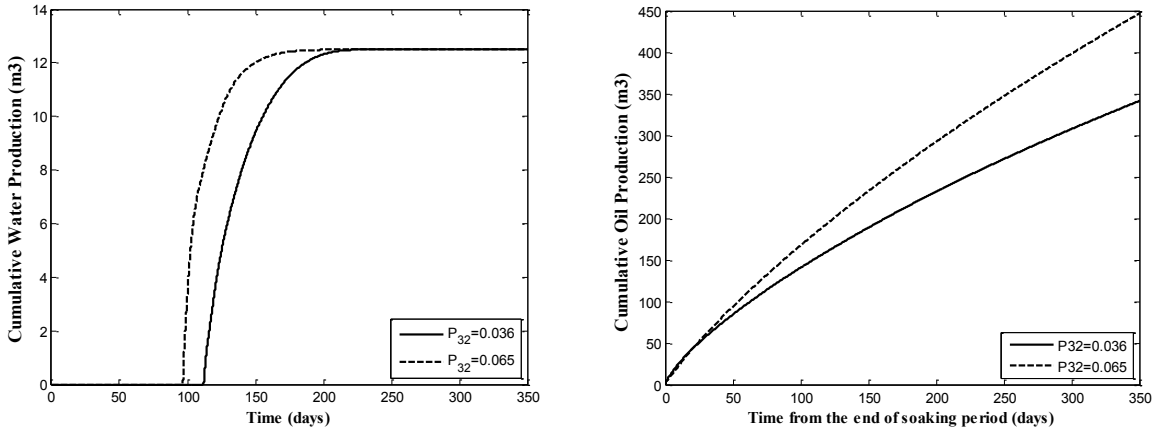

Fig. 4. 11. Water and oil production profiles for two cases with same water flow-back amount but different NF properties

4.1.2 Impact of Matrix Irreducible Water Saturation

In certain tight reservoirs, matrix is desiccated (initial water saturation is less than irreducible water saturation). A number of reasons including compaction, dehydration, disconnection of oil reservoir from free water level and diagenesis have been cited (Bennion *et al*., 2002; Gupta 2009). Generally speaking, as wettability to water increases, initial water saturation increases; however, desiccated reservoir can also be water wet, and the Cardium formation is an example of a desiccated water-wet reservoir, as evidenced by its low initial water saturation and oil relative permeability end point being higher than its corresponding water relative permeability end point (Purvis *et al*., 1979; Coskuner 2006). Experimental study of Coskuner (2006) also confirms that water-based fracturing fluid may cause water blockage near hydraulic fracture in desiccated tight reservoir and hamper oil/gas production. Similar observations are obtained from the numerical study of Assiri *et al*. (2014), although their model did not include a fracture system. Therefore, the influence of matrix desiccation on matrix imbibition, water trapping in matrix, water flow-back and oil production in fractured tight oil reservoir is investigated in this section. Three cases with different irreducible water saturations (S_{wirr} = 0.25, 0.3, 0.4) are constructed. Other parameters, including initial water saturation, are the same as the base case.

Water saturation profiles around secondary fractures for different cases during shut-in are presented in **Fig. 4.12**. Imbibed water is trapped in the matrix near the fractures up to the irreducible water saturation level. It cannot advance further into the matrix due to zero mobility; as a result, relative mobility to oil is decreased due to the increased water saturation, which has a negative impact on oil production (**Table 4.3**). As shown in **Table 4.3**, matrix imbibition during shut-in increases with desiccation, causing more water loss. This is evidenced by the decreased water recovery (as compared to the base case, of 8.82%, 15.99% and 23.09% for the cases with

S_{wirr} = 0.25, 0.3, 0.4, respectively).

Table 4. 3 Oil and water production for desiccated matrix system

S_{wirr}	$Q_{o1000\text{days}}$ (m^3)	$Q_{w1000\text{days}}$ (m^3)
0.2	571.94	13.38
0.25	571.37	12.20
0.3	569.69	11.24
0.4	564.61	10.29

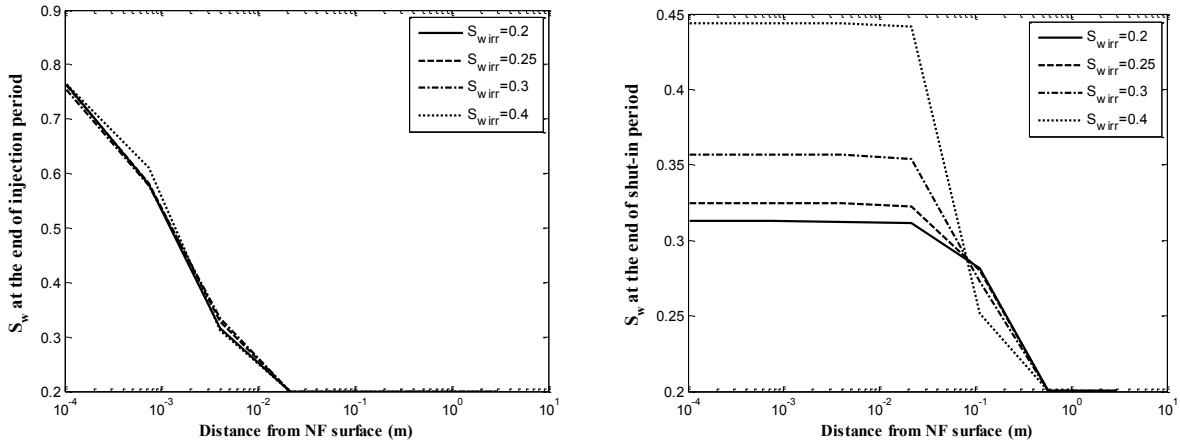

Fig. 4. 12. Water saturation profiles in desiccated matrix at the end of shut-in

4.2 Water Retention in Secondary Fractures

Pagels *et al*. (2012) and Fan *et al*. (2010) proposed that high capillary pressure caused by small permeability and aperture can cause water trapping in the secondary fractures. The concept of permeability jail has also been proposed by some researchers as a possible mechanism for water

trapping in secondary fractures (Shanley *et al*., 2004; Wattenbarger *et al*., 2013). Detailed understanding of how secondary fracture and matrix properties can influence water retention in secondary fractures is still unclear. In this section, the influences of secondary fracture properties, matrix properties and injection rate on water retention in secondary fracture are investigated. A new dimensionless capillary number is formulated to correlate the interplay between viscous and capillary forces to imbibition and water recovery for a given matrix-fracture system.

4.2.1 Impact of Secondary-Fracture Conductivity

A series of models with varying secondary-fracture permeability (k_{NF} = 100mD, 5mD) and matrix permeability (k_M = 0.0005mD, 0.0017mD, 0.0025mD), but with constant fracture pore volume, are simulated, and their corresponding water saturation profiles are presented in **Fig. 4.13**. When k_{NF} is small (e.g., 5mD), as k_M increases, both matrix capillary pressure and imbibition decrease. Lower k_{NF} is also accompanied by higher capillarity in secondary fracture, which has a negative impact on matrix imbibition. However, it is interesting to note that the trend is more complicated when k_{NF} is large (e.g., 100mD): upon shut-in, as k_M increases, imbibition rate increases; however, this trend is slowly reversed as shut-in continues. This observation may be explained with the saturation equation (Eq. 4.2) commonly implemented in finite-difference simulators (Ertekin *et al*., 2001), in which total compressibility (~ 1×10^{-9} Pa^{-1}) is ignored. During the early times upon shut-in, high k_{NF} and $T_{F\text{-}M}$ contribute to an increased water flow into the matrix and higher water saturation (lower capillary pressure) in regions near the secondary fracture. This is a scenario where viscous force is dominant; therefore, as k_M increases, imbibition rate increases. However, as imbibition progresses deeper into the matrix at late times,

water saturation in the regions neighboring the secondary fracture would decrease, allowing capillary pressure to increase (i.e., imbibition becomes capillarity-driven); therefore, as k_M increases, imbibition drops. The impact of secondary fracture conductivity on imbibition and flow-back is investigated by varying fracture permeability k_{NF} (100mD, 10mD, 5mD, 3mD) and their corresponding capillary pressure functions. As shown in **Fig. 4.14**, as k_{NF} decreases, capillary pressure and water saturation in secondary fracture increase as matrix imbibition decreases. Two observations can be drawn from the production profiles in **Fig. 4.15** as k_{NF} decreases: 1) water recovery increases, since less water is imbibed into the matrix; and 2) more water is retained in the secondary fracture during flow-back, so oil production decreases. An important implication is that despite the increase in water saturation in secondary fracture, there is no mechanism to trap the retained water. It is observed, however, that lower NF conductivity would slow down matrix imbibition.

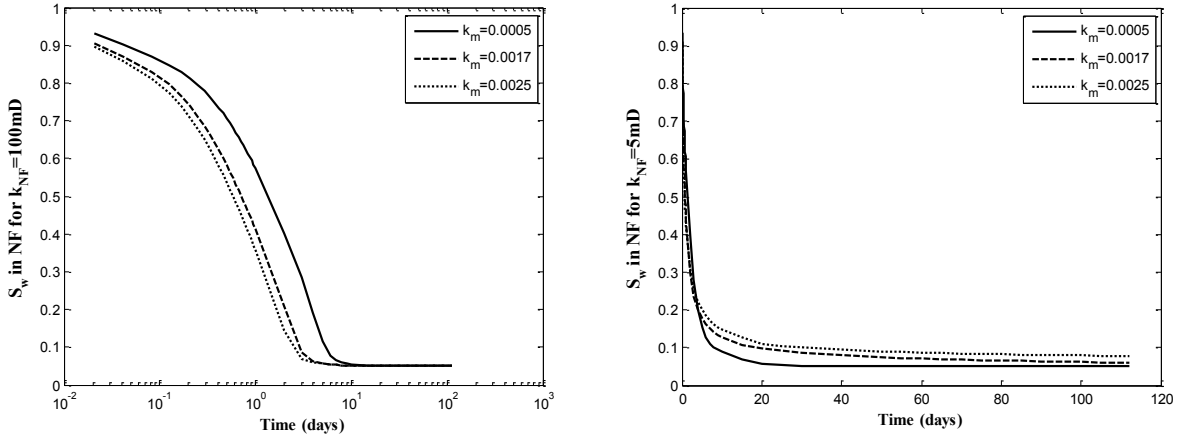

Fig. 4. 13 Water saturation profiles in secondary fracture for different k_M

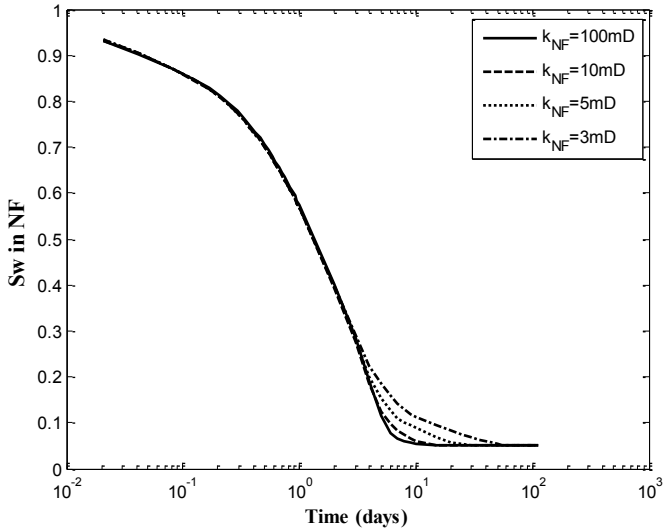

Fig. 4. 14 Water saturation profiles in secondary fracture during shut-in as a function of k_{NF}

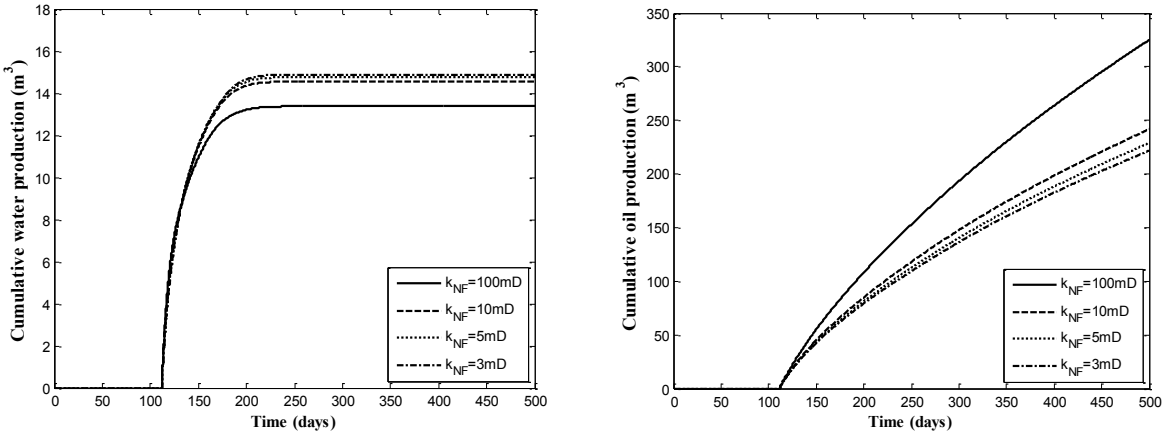

Fig. 4. 15 Water and oil production profiles for different k_{NF}

4.2.2 Interaction between Viscous and Capillary Driving Forces

For a given porous structure, imbibition is known to be a function of a general dimensionless capillary number (N_{Ca}) defined as the ratio of the viscous to the capillary forces (Eq. 4.3) in Peters (2012). For naturally-fractured reservoirs, Putra *et al*. (1999) proposed a "Fracture

Capillary Number" or N_{fCa} (Eq. 4.4), which reflects the relative magnitudes of viscous force along the fracture and capillary force perpendicular to the fracture surface. However, this formulation of N_{fCa} assumes that viscous force exists only in the fracture, while capillary force exists only in the matrix. Although this assumption is generally valid during water-flooding, it does not hold during shut-in and flow-back; this is because velocity in fracture during shut-in is very low; hence both viscous and capillary forces would contribute to the fluid exchange between fracture and matrix. The objective here is to (1) formulate a dimensionless N_{Ca} to illustrate the interaction between viscous and capillary forces, and (2) assess and correlate its impacts on imbibition and fluid recovery during shut-in and flow-back.

$$N_{Ca} = \frac{v \cdot \mu'_w}{\sigma'} \quad \text{..... (4.3)}$$

$$N_{fCa} = \frac{9.05 \times 10^{-5} q_{inj} \cdot \mu'_w}{\frac{P_{c,\max}}{J(S_{wi})} \sqrt{\frac{k_M}{\varphi_M}} A_M} \quad \text{..... (4.4)}$$

To evaluate the sensitivity to viscous driving force, two cases with different water injection rates ($60m^3$/day, $100m^3$/day) are modeled. Water saturation profiles in hydraulic and secondary fracture during shut-in are shown in **Fig. 4.16**, and the corresponding production data is shown in **Table 4.4**. The results indicate that as injection rate and fluid pressure in fracture at the end of injection period increase, water retention in fracture increases and water saturation in fracture remains high during shut-in, enhancing water production while hampering initial oil production during flow-back. To evaluate the sensitivity to capillary driving force, two cases with different interfacial tensions in the matrix (20 dyne/cm, 25 dyne/cm) are modeled. Water saturation profiles in hydraulic and secondary fractures during shut-in are presented in **Fig. 4.17**, and the corresponding production data is shown in **Table 4.5**. The results indicate that as interfacial

tension and capillary pressure increase, imbibition is enhanced, which leads to lower water recovery and improved oil recovery.

Table 4. 4 Oil and water production for different injection rate cases

q_{inj}	Oil rate (1 day)	Water rate (1 day)	$Q_{o500\text{days}}$	$Q_{w500\text{days}}$
60 m^3/day	2.20 m^3/day	0.88 m^3/day	325.03m^3	12.74m^3
90 m^3/day	2.15 m^3/day	0.93 m^3/day	324.74m^3	13.38m^3
100 m^3/day	2.14 m^3/day	0.94 m^3/day	324.64m^3	13.59m^3

Table 4. 5 Oil and water production for different interfacial tensions

σ'	Oil rate (1 day)	Water rate (1 day)	$Q_{o500\text{days}}$	$Q_{w500\text{days}}$
20dyne/cm	1.86 m^3/day	1.29 m^3/day	321.78m^3	19.61m^3
25dyne/cm	2.01 m^3/day	1.10 m^3/day	323.32m^3	16.30m^3
30dyne/cm	2.15 m^3/day	0.93 m^3/day	324.74m^3	13.38m^3

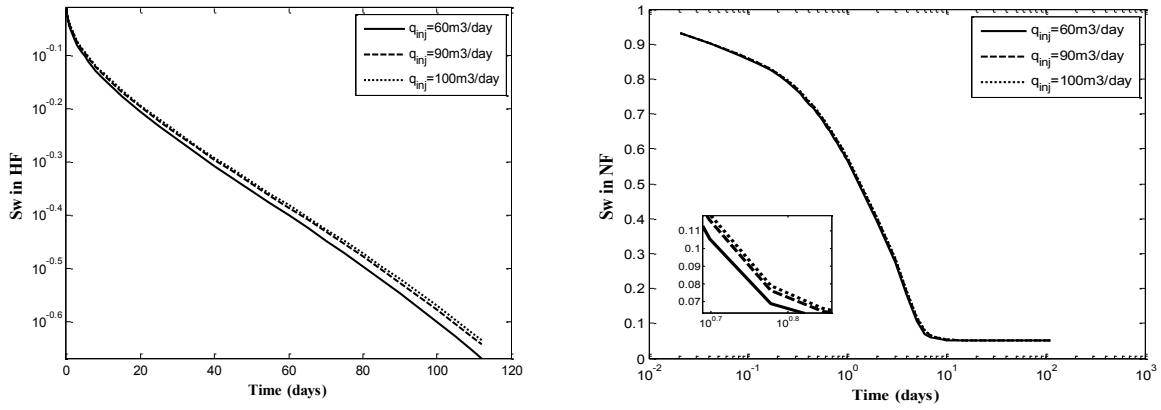

Fig. 4. 16 Water saturation profiles in HF and NF during shut-in for different water injection rates

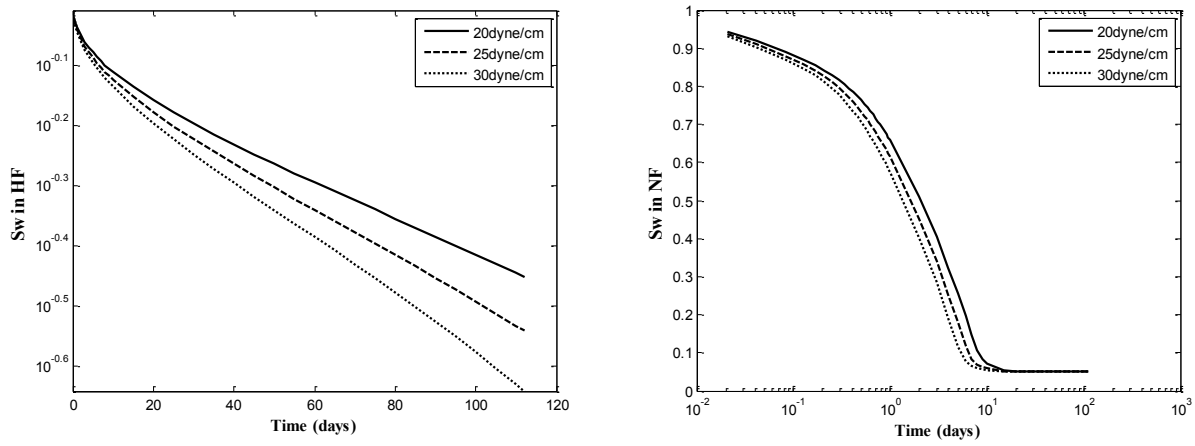

Fig. 4. 17 Water saturation profiles in HF and NF during shut-in for different interfacial tensions

Based on the aforementioned observations, the following dimensionless capillary number is modified from Putra *et al*. (1999) to evaluate the efficiency of matrix imbibition under the impacts of viscous and capillary forces (Eq. 4.5):

$$N_{Ca} = \frac{q_{inj} \cdot \mu'_w}{\sigma' \cdot A_M} \quad \text{.....(4.5)}$$

Where q_{inj} is water injection rate, μ'_w is water viscosity, σ' is interfacial tension between water and oil, and A_M is the contact area between fracture and matrix. As N_{Ca} increases, matrix imbibition decreases, which results in more water retention in fracture and higher water recovery. The values of N_{Ca} and water recovery from different cases are presented in **Fig. 4.18**. The results here indicate that lower injection rate (and lower shut-in pressure in fracture) may reduce water recovery and enhance oil production.

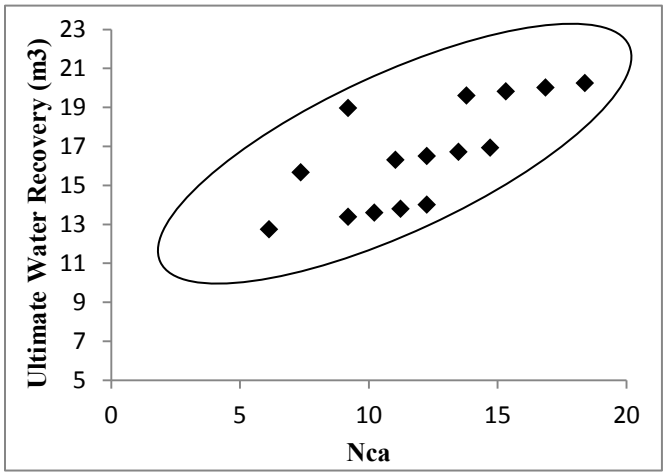

Fig. 4. 18 Relationship between N_{ca} and water recovery

4.2.3 Impact of Permeability Jail

Shanley *et al*. (2004) proposed the concept of permeability jail in tight rocks, where over a range of saturation that neither wetting nor non-wetting phase can flow. The authors postulated that overburden stress could reduce fluid effective permeability in tight reservoirs by several orders of magnitude, which is the reason for the permeability jail. Despite this phenomenon has not been validated by many laboratory experiments, it is still enlightening to explore the effect of permeability jail considering that overburden stress could be significant in many tight reservoirs. Capillary pressure under permeability jail case is higher than that in conventional rocks (Shanley *et al*., 2004). Relative permeability and capillary pressure functions representative of the permeability jail scenario are shown in **Fig. 4.19**. Other parameters are the same as base case. It is observed that water saturation in secondary fractures remain high during shut-in because little water has imbibed into the matrix. The reason is that once the water saturation in the matrix surrounding the connected fractures has reached the two-phase immobile range, counter-current

imbibition would cease. As a result, water saturation increases and oil-phase relative permeability decrease in the secondary fractures. This is evidenced by the decreased initial oil production and increased initial water production in **Fig. 4.20**.

Table 4.6 presents the water and oil production data for different shut-in durations (1 day, 2 weeks and 6 weeks) in the presence permeability jail. In contrast to the results in 4.1.1, prolonged shut-in would decrease the cumulative oil production. Although as shut-in continues, less water is flown back; however, more water would be imbibed into matrix, creating an enlarged two-phase immobile region in the matrix near the connected fractures, impacting adversely on the ultimate recovery. Therefore, shortened shut-in duration is beneficial for oil production if formation exhibits permeability jail condition.

Table 4. 6 Oil and water production for different shut-in durations in the presence of permeability jail

Shut-in Duration	$Q_{o300\text{days}}$ (m^3)	$Q_{w300\text{days}}$ (m^3)
1 day	19.47	13.80
6 weeks	14.55	13.47
16 weeks	13.25	13.26

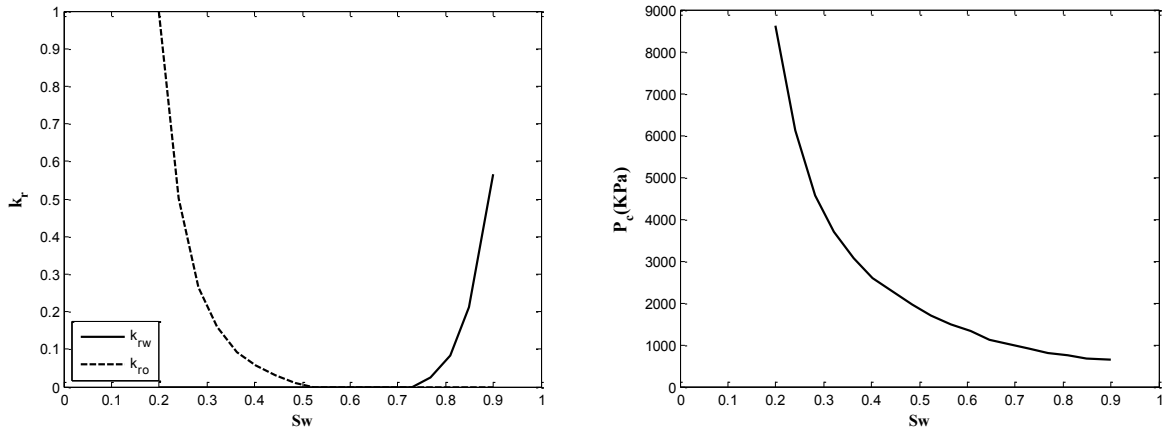

Fig. 4. 19 Matrix relative permeability and capillary pressure functions representing the permeability jail

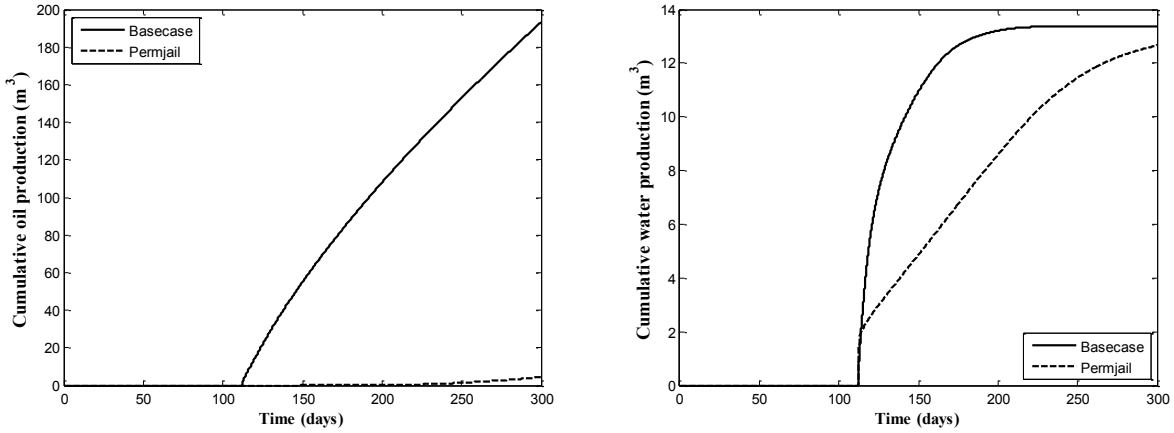

Fig. 4. 20 Water and oil production profiles in the presence of permeability jail

4.3 Discussion

A detailed numerical model is constructed to simulate multiphase flow in fractured media during flow-back operation. The model is built using commercially-available black-oil simulator, and the applicability of the attained results has been validated against published field data in the literature. The novelties of this model include: 1) water leak-off during fracturing fluid injection period is incorporated to reflect realistic fracturing fluid efficiency; 2) sensitivity of pressure distribution at the end of injection period is studied to understand the potential implications on operational strategies; 3) integration of stochastic discrete fracture network provides improved representation of realistic fracture heterogeneity; and 4) coupling of matrix/fracture properties and multiphase flow functions has been fully considered.

An important message is that water transport between fracture and matrix during shut-in period depends on the interplay of viscous and capillary fluxes. In many instances, higher initial rate does not guarantee improved long-term recovery. A number of factors including properties of matrix and fractures or shut-in duration are important considerations.

Two possible water-loss mechanisms are investigated in this paper: matrix imbibition and water retention in secondary fractures. In terms of matrix imbibition, Cheng (2012) and Fakcharoenphol *et al*. (2013) indicated that prolonged shut-in duration would improve initial oil/gas production rate, a similar observation is also observed. In addition, the influences of fracture network properties (fracture length, fracture intensity and fracture connectivity) on matrix imbibition, which has not been studied previously, are presented in this study. The results indicate that as fracture-matrix contact area increases, matrix imbibition and water loss increases. Therefore, it is concluded that although matrix imbibition may enhance initial production rate, secondary fractures are required to enhance long-term production. Furthermore, time scale

associated with matrix imbibition is crucial. An important observation is that water is not trapped indefinitely in the matrix (except when matrix is desiccated or permeability jail exists); however, high initial rate can result from prolonged shut-in, while actual long-term enhancement in production can only be attributed to extensive connected secondary fracture networks.

We have also investigated factors that would increase water saturation in secondary fractures. Results indicate that lower fracture conductivity would slow down matrix imbibition and increase water saturation in fractures; this result is in agreement with Wattenbarger *et al*. (2013). However, other aspects of this study's observations are different: assigning same relative permeability functions in both matrix and secondary fractures, they concluded that lower relative permeability in both matrix and secondary fractures would reduce matrix imbibition and higher matrix capillary pressure can enhance imbibition. Although this study confirms that lower permeability in secondary fractures would reduce imbibition rate, impact of matrix permeability, yet, depends on the relative magnitudes of viscous and capillary fluxes. Wattenbarger *et al*. (2013) also concluded that higher matrix capillary pressure can enhance imbibition; however, capillary pressure was varied independently of matrix permeability. In this work, matrix capillary pressure function is assigned in accordance to matrix permeability, and the impacts of viscous and capillary forces are captured in the proposed dimensionless capillary number (N_{Ca}). Although similar capillary number has been used in previous water-flooding study (Qasem *et al*., 2008), its formulation and interpretation here are different. In contrast to water-flooding, flow parallel to fracture plane during shut-in is negligible, and the assumption of viscous-driven flow in fracture and capillary-driven flow in matrix is inaccurate. This study also corroborates previous studies that permeability jail would increase water saturation in natural fracture with an adverse effect on production. In general, various factors including matrix permeability,

secondary-fracture permeability and initial fracture pressure can contribute to higher water saturation in secondary fractures at the end of shut-in by reducing water imbibition rate, but this water can be flown back upon production. This conclusion, though differs from Fan *et al*. (2010) and Pagel *et al*. (2012), which suggested that water retained in low conductivity fracture is trapped permanently, provides important insight regarding the role of secondary fracture in water retention and imbibition time-scale.

Chapter 5: Effect of Multiphase flow and Geomechanics on Flow Back Operation

5.1 Matrix Wettability

An increase in wettability to water is typically accompanied by increases in water-oil capillary pressure and oil relative permeability and a decrease in water relative permeability; as a result, the initial water saturation increases. As discussed in the introduction, the coupled effect of multiphase flow functions and initial water saturation as a function of wettability on imbibition in matrix and secondary fracture systems is not well understood. In this section, the impacts of individual components and their combined effects are systematically investigated.

5.1.1 Impact of Water-oil Capillary Pressure and Relative Permeability Functions

In addition to the base case, two different water-oil capillary pressure functions, as presented in **Fig. 5.1** (Case 1 and Case 2), are tested, where $P_{c\ base\ case} > P_{c\ case\ 1} > P_{c\ case\ 2}$. The corresponding water saturation profiles in the hydraulic and secondary fracture systems during shut-in period are presented in **Fig. 5.2**, while the water and oil production results are summarized in **Table 5.1**. As expected, water-oil capillary pressure enhances matrix imbibition and water loss because less water is retained in the fractures at the end of soaking period. Although this counter-current imbibition might improve initial oil flow rate, there is no observable benefit in long-term oil

production. Next, the sensitivity of water-oil relative permeability functions is tested. Two different water-oil relative permeability functions (Case3 and Case 4), as shown in **Fig. 5.1**, are tested, where $k_{rw\ base\ case} < k_{rw\ case\ 3} < k_{rw\ case\ 4}$ and $k_{ro\ base\ case} > k_{ro\ case\ 3} > k_{ro\ case\ 4}$. The corresponding water saturation profiles in the hydraulic and secondary fracture systems during shut-in period are presented in **Fig. 5.3**, while the water and oil production results are summarized in **Table 5.1**. It is clear that reduction in water relative permeability hampers imbibition; therefore, more water is retained in the fractures, causing the initial oil rate to drop and initial water rate to rise. It is interesting to note that, despite the lower initial oil rate, long-term oil production is improved due to the higher oil relative permeability, while long-term water recovery is also increased because of reduced water loss.

Table 5. 1 – Summary of water and oil production for the base case, Case 1-15 and A-D

	Initial rate (SC) (m^3/day)		**Cumulative production over 300 days (RC) (m^3)**		**Remarks**	
	oil	**water**	**oil**	**water**		
Base Case	2.15	0.93	193	13.38	--	
Case 1	1.94	1.19	191	17.83	Sensitivity of capillary pressure functions	
Case 2	1.70	1.49	190	22.93		
Case 3	2.26	0.83	185	12.11	Sensitivity of relative permeability functions	
Case 4	2.31	0.77	176	11.51		
Case 5	2.03	1.10	183	16.72	Combination of Cases 1 & 3	
Case 6	1.79	1.37	172	21.64	Combination of Cases 2 & 4	
Case 7	1.89	1.13	173	17.24	Sensitivity of S_{wi}	
Case 8	1.63	1.33	152	21.32		
Case 9	1.16	1.68	114	30.05		
Case 10	1.63	1.33	152	21.32	Coupling of multiphase functions and S_{wi}	
Case 11	1.77	1.30	164	20.58		
Case 12	1.79	1.37	172	21.64		
Case 13	1.93	0.55	175	8.70	P_{wf} = 35MPa	Stiff formation
Case 14	1.81	0.70	166	11.91	Coupling of geomechanics with multiphase flow functions	
Case 15	1.60	0.94	155	16.72		
Case A	2.53	0.32	141	6.39	No secondary fractures	
Case B	2.53	0.32	144	6.40	Disconnected oil-filled fractures	
Case C	2.53	0.32	144	6.40	Disconnected water-filled fractures	
Case D	3.15	0.41	428	2.77	Connected fractures	

Table 5. 2 – Summary of water, oil and gas production for Case 13, 16-23

	Initial rate (SC) (m^3/day)			Cumulative production over 300 days (SC) (m^3)			Remarks	
	oil	gas	water	oil	gas	water		
Case 13	1.93	193	0.55	132	13173	6.66	P_{wf} = 35MPa	Stiff formation
Case 16	4.06	595	1.45	325	30650	14.50	P_{wf} = 10MPa	
Case 17	4.23	660	1.59	345	33075	15.30	P_{wf} = 5MPa	
Case 18	0.99	99	0.30	78	7795	4.50	P_{wf} = 35MPa	Medium formation
Case 19	1.24	141	0.42	103	10173	5.73	P_{wf} = 10MPa	
Case 20	1.25	143	0.43	104	10288	5.78	P_{wf} = 5MPa	
Case 21	0.69	69	0.22	57	5730	3.71	P_{wf} = 35MPa	Soft formation
Case 22	0.76	79	0.26	64	6335	4.06	P_{wf} = 10MPa	
Case 23	0.76	79	0.26	64	6340	4.06	P_{wf} = 5MPa	

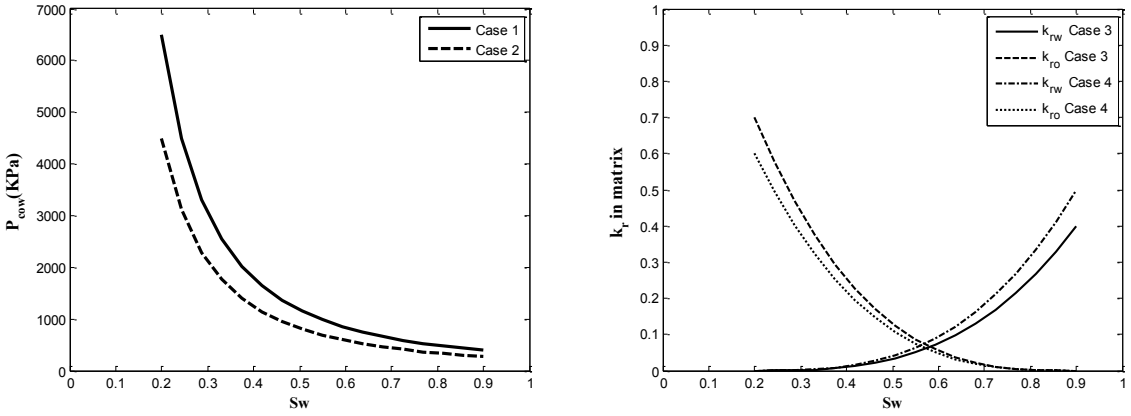

Fig. 5. 1 Matrix multiphase flow functions for the different cases

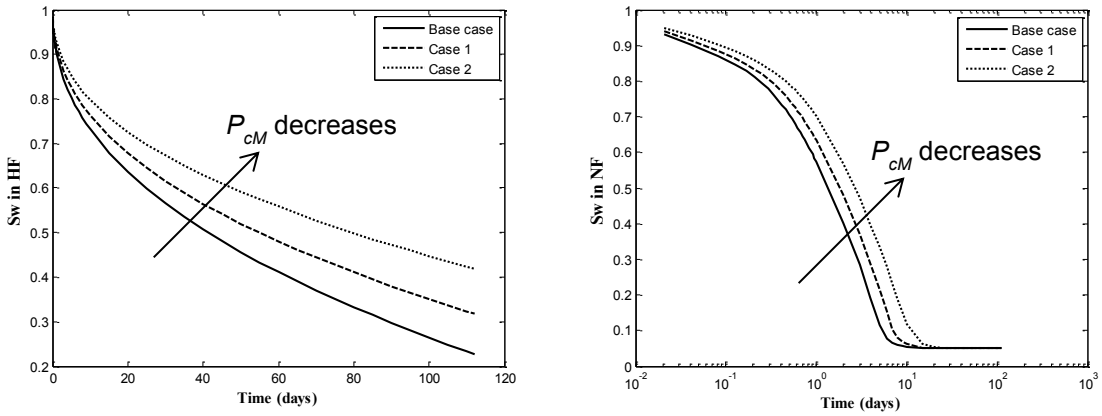

Fig. 5. 2 Profiles of water saturation in fractures corresponding to different matrix capillary pressure functions

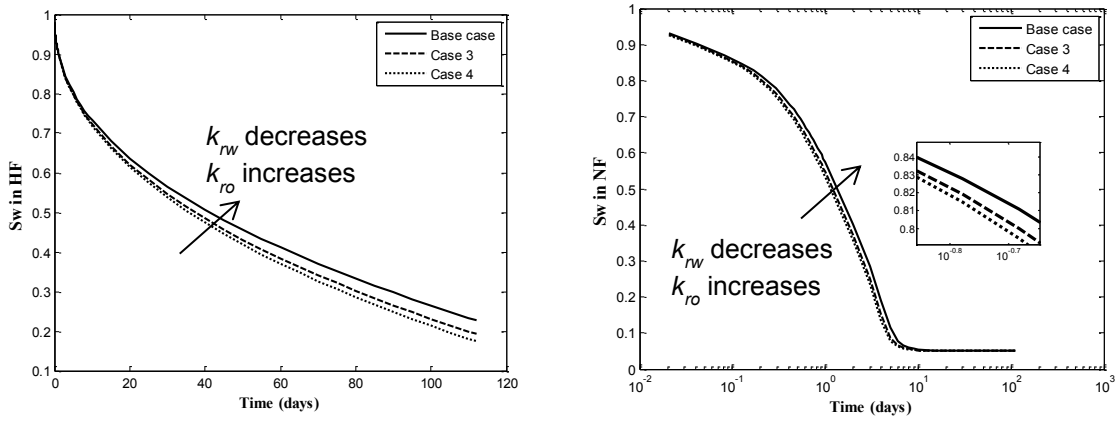

Fig. 5. 3 Profiles of water saturation in fractures corresponding to different relative permeability functions in matrix

Although it is important to understand the impacts of water-oil capillary pressure and relative permeability individually, these functions, however, depend on the system wettability and should be modeled in a coupled manner. The premise for coupling these functions is that as matrix becomes more water wet, water-oil capillary pressure and oil relative permeability increase, while water relative permeability decreases. Therefore, Case 5 is constructed by combining the

water-oil capillary pressure function of Case1 with the water-oil relative permeability functions in Case 3 to represent a more water-wet scenario, while Case 6 is constructed by combining the water-oil capillary pressure of Case 2 and water-oil relative permeability of Case 4 to represent a less water-wet scenario. In other words, $P_{c\ base\ case} > P_{c\ case\ 5} > P_{c\ case\ 6}$, $k_{rw\ base\ case} < k_{rw\ case\ 5} < k_{rw\ case\ 6}$, and $k_{ro\ base\ case} > k_{ro\ case\ 5} > k_{ro\ case\ 6}$. The ensuing water saturation profiles in the fracture systems during shut-in period are compared in **Fig. 5.4**, and the corresponding water and oil production information are illustrated in **Table 5.1**. The results suggest that imbibition is higher for the more water-wet case; as a result, less water is retained in the fracture at the end of the soaking period. This, in turn, has led to lower water recovery (more water loss). Both the initial and cumulative oil productions are higher due to (1) higher oil relative permeability and (2) enhanced counter-current imbibition.

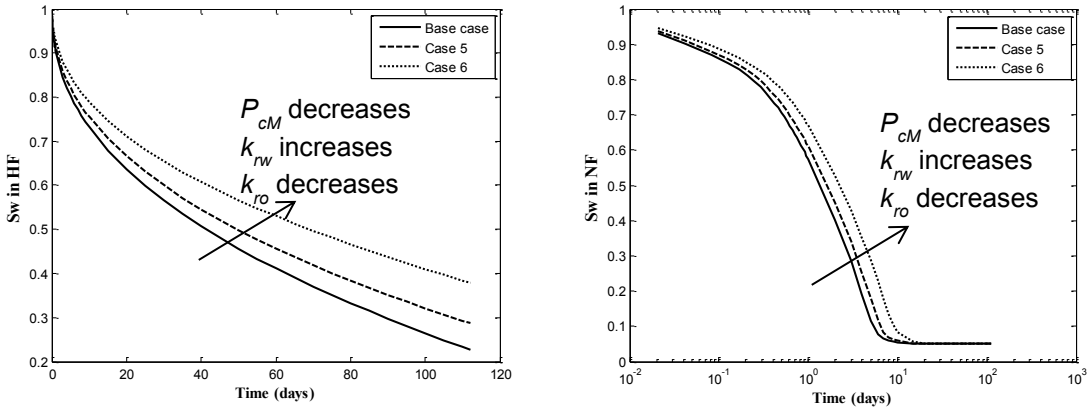

Fig. 5. 4 Profiles of water saturation in fractures corresponding to different multiphase flow functions in matrix

A few conclusions can be drawn from this analysis of water-oil system: 1) despite both capillary pressure and relative permeability may influence imbibition, capillary pressure appears to have a

more dominant effect when the two factors are coupled; 2) imbibition improves the initial oil rate but hinders water recovery; and 3) the cumulative oil production is highly influenced by oil relative permeability. Given that there is no direct correlation between high initial oil flow rate and improved cumulative oil production, in order to enhance the long-term production, measures, including addition of surfactant to fracturing fluids (Liang *et al*., 2015) for increasing oil relative permeability should be considered.

5.1.2 Impact of Initial Water Saturation

A positive relationship between wettability and initial water saturation (S_{wi}) is commonly observed, as evidenced by the experimental data of Jadhunandan *et al*. (1995) and Bennion *et al*, (2002). Sensitivity of the flow-back behavior due to initial water saturation is analyzed here. Three cases with different initial water saturations (Case 7: S_{wi} = 0.25, Case 8: S_{wi} = 0.3, Case 9: S_{wi} = 0.4) are compared. In this section, the capillary pressure and relative permeability functions are assumed to be the same as those of the base case. The corresponding profiles of water saturation in the fracture systems and the production information are shown in **Fig. 5.5** and **Table 5.1**, respectively. Imbibition decreases with S_{wi} because there is less pore space for the imbibed water. This trend would eventually lead to higher water recovery and lower oil production.

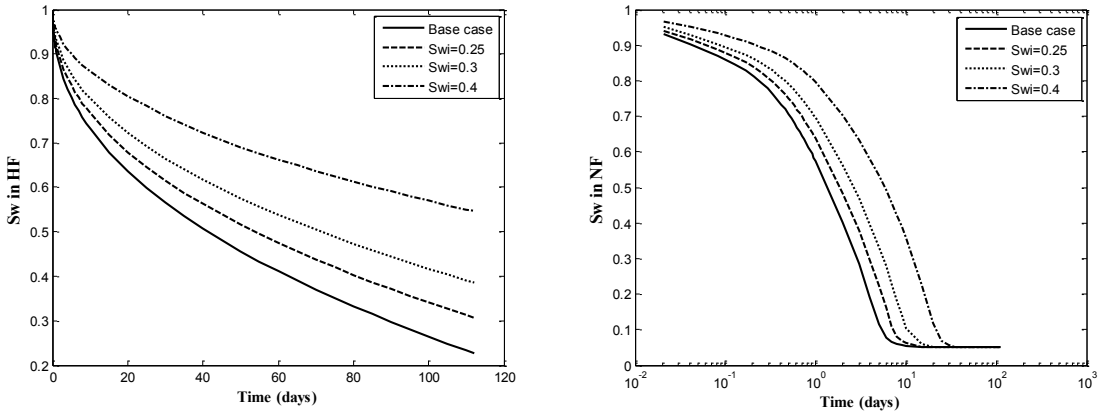

Fig. 5. 5 Profiles of water saturation in fractures corresponding to different S_{wi} (Cases 7-9)

5.1.3 Coupling of Multiphase Flow Functions and Initial Water Saturation – Effects of Wettability in an Water-Oil System

Individual effects of water-oil multiphase flow functions and S_{wi} are studied in the previous sections; however, these two components should vary in accordance to system wettability. With the general understanding that S_{wi} is higher in a more water-wet formation, three new cases are compared: Case 10 combines the base case with S_{wi} = 0.3 (most water-wet); Case 11 combines Case 5 with S_{wi} = 0.25 (medium water-wet); and Case 12 combines Case 6 with S_{wi} = 0.2 (least water-wet). The corresponding water saturation profiles in the fracture systems and the production information are presented in **Fig. 5.6** and **Table 5.1**. It is interesting to note that imbibition is most significant in Case 11; the reason for a lack of direct or linear relationship between wettability and imbibition is that with stronger wettability, both capillarity and S_{wi} would increase, with opposing influences on imbibition. Ultimately, imbibition and flow-back performance depends on the interplay between water-oil multiphase flow functions and S_{wi}. A generalization of their overall impacts would be impractical. Therefore, uncertainty assessment regarding their impacts should be performed in a coupled manner that takes into account of

wettability for a given formation.

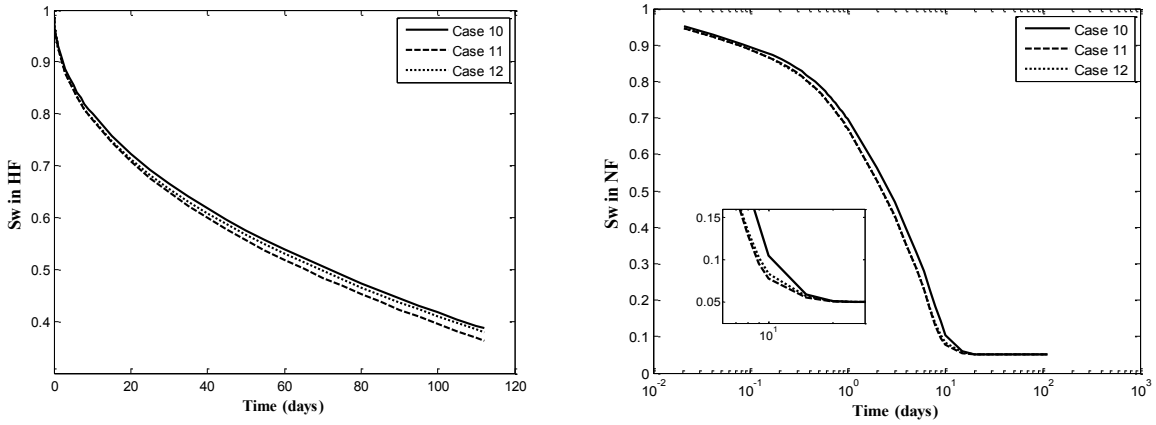

Fig. 5. 6 Profiles of water saturation in fractures corresponding to different matrix wettability

5.2 Stress-Dependent Fracture Conductivity

As water imbibes into the matrix during shut-in, the fluid pressure in the fracture decreases; as a result, the effective stress inside the fracture increases, causing the fracture conductivity to decrease. During the flow-back phase, pressure inside the fracture continues to decline, and the fracture conductivity is reduced further. The impact of stress-dependent fracture conductivity on fracturing fluid flow-back is studied next.

Case 13 is constructed using the stress-dependent fracture conductivity relationship for a stiff formation (Eq. 3.8 and Eq. 3.10), and the results are compared in **Figs. 5.7-5.8** and **Table 5.1**. Both short-term and long-term water and oil productions are reduced when fracture compaction is considered. It is interesting to note that despite fracture compaction may enhance counter-current imbibition, as indicated in the saturation profile in **Fig. 5.8**, the initial oil flow rate

actually decreases as a result of reducing fracture conductivity (**Table 5.1**), which, in addition to increased water loss, also contributes to the decreased water production. It should be noted that the conclusions derived in this section may be applicable only for a strong set of secondary fractures, as modeled in this study, that are approximately orthogonal to each other,.

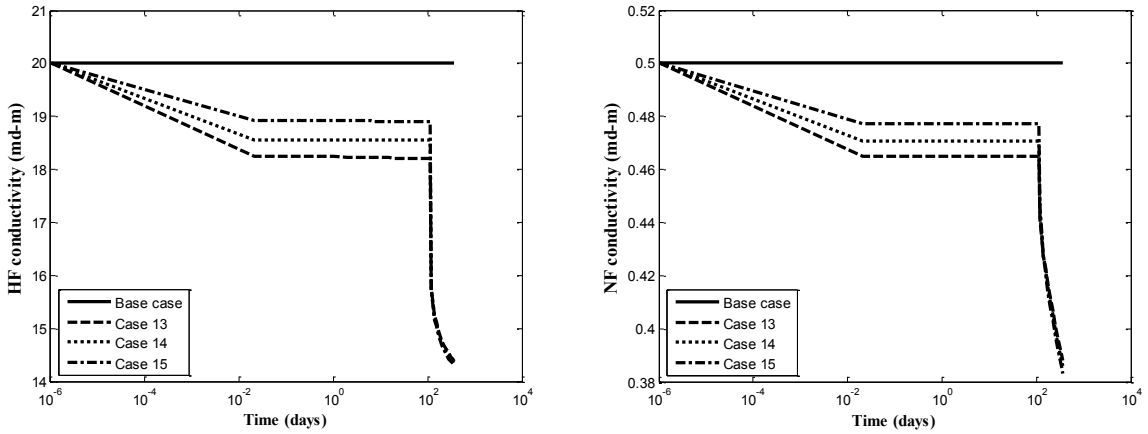

Fig. 5. 7 Comparison of stress-dependent fracture conductivity profiles during shut-in and production periods

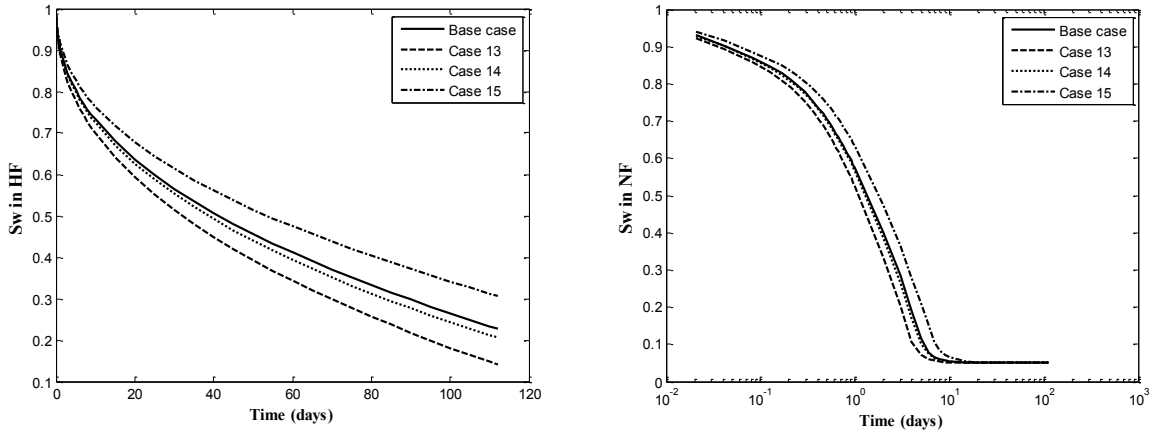

Fig. 5. 8 Profiles of water saturation in fractures considering stress-dependent fracture conductivity

5.2.1 Coupling with Water-Oil Multiphase Flow Functions

The combined effects of water-oil multiphase flow functions and fracture compaction on imbibition and fluid recovery is investigated next. The stress-dependent fracture conductivity relationship from the previous section is combined with the water-oil multiphase flow functions from Cases 5 and 6 to construct Cases 14 and 15, respectively. Variations in fracture conductivity during the shut-in and production phases for all cases are compared in **Fig. 5.7**. The corresponding water saturation profiles and production results are presented in **Fig. 5.8** and **Table 5.1**. The results indicate that the impacts of improved imbibition in water-wet matrix are two folds: first, water recovery decreases and oil production increases (see section 4.1.1); second, it could lead to more fracture compaction, which, as noted previously, could have potential negative impacts on both water and oil productions due to reduced fracture conductivity. For this particular study, the consequence of these two offsetting aspects is an increased oil production. The results underline an important insight that matrix imbibition leads to more fracture compaction, which, in turn, enhances imbibition and water loss. Reduction in fracture conductivity has a definite negative impact on water production; however, this similar negative impact on oil production may be counteracted by the benefits of improved counter-current imbibition and possibly higher oil relative permeability in water-wet rocks.

5.2.2 Impacts of Bottom-Hole Pressure and Solution Gas

It is typically expected that as bottom-hole pressure (P_{wf}) decreases, both water clean-up and oil production are improved due to the increased drawdown and the additional solution gas drive below the bubble-point pressure. However, declining P_{wf} could also lead to fracture compaction,

which, as shown previously, could have adverse effects on water recovery and oil production. To illustrate this hypothesis, three different P_{wf} levels (35 MPa, 10 MPa, 5 MPa) are tested. In addition to Case 13 with P_{wf} = 35MPa, Cases 16-17 are constructed with P_{wf} = 10 MPa and 5 MPa, respectively. Two similar sets, Cases 18–20 and 21–23, are created for the medium and soft formations, respectively. Variations in fracture conductivity during shut-in and production periods for all cases are illustrated in **Fig. 5.9**, and the corresponding production information is compared in **Table 5.2**. For a given P_{wf}, as rock stiffness decreases, fracture conductivity decline during shut-in and production period is more prominent. It is very interesting to note that although decreasing P_{wf} would improve water recovery and oil production, particularly for stiff rock, this improvement, however, is not as obvious for medium and soft rocks due to excessive fracture closure at low P_{wf}; as evidenced in Cases 19-20 and 22-23. This observation has significant implications on operations design: aggressive flow-back is helpful on water recovery and oil production for stiff formations; however, this benefit is less prominent in medium to soft formations, which are more prone to fracture closure.

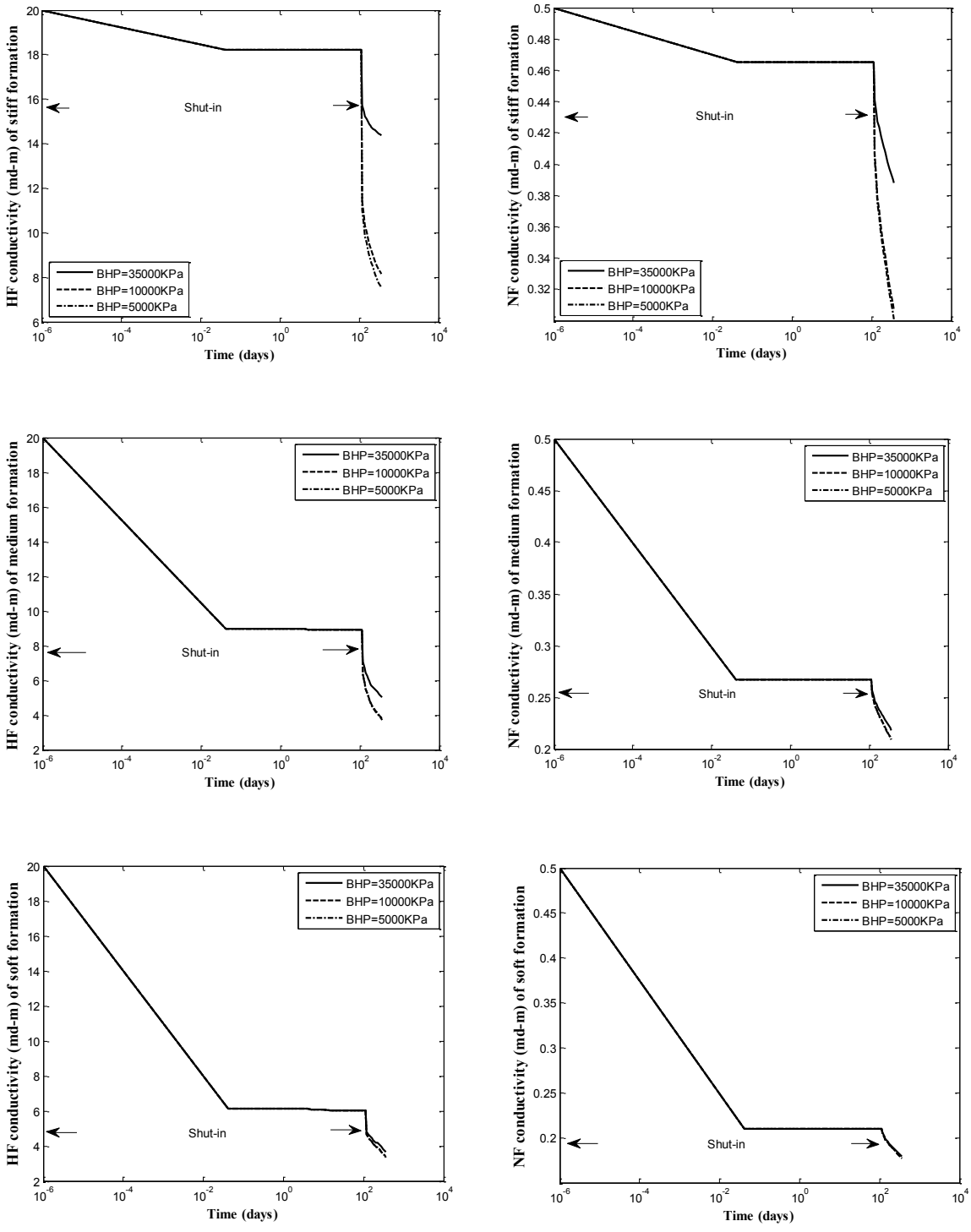

Fig. 5. 9 Comparison of stress-dependent fracture conductivity profiles during shut-in and production periods for Cases 13, 16-23 with different P_{wf} and E

The impact of bottom-hole pressure on solution gas and gas production is also summarized in **Table 5.2**. Similar to the trends of oil production, the improvement in gas production with reduced P_{wf} is less noticeable in soft formations than in stiff formations due to fracture closure. It has been reported in the literature that the bubble-point pressure would decrease with formation pore radius reduction in tight rocks (Nojabaei, *et al*. 2013). In such cases, less gas would evolve from the oil during the production phase; hence, the impacts on gas production could be less important in actual reservoir settings.

5.2.3 Impact of Gas Relative Permeability

Three different gas relative permeability end points are tested, and the results for different formation stiffness are listed in **Table 5.3**. It appears that increasing the gas relative permeability would enhance the cumulative gas production slightly, while influences on both the oil and water production are negligible. This observation is most obvious in stiff formation, similar to the findings in previous sections.

Table 5. 3 – Summary of water, oil and gas production for Case 16, 19, 22, 24-29

	Initial rate (SC) (m^3/day)			**Cumulative production over 300 days (SC) (m^3)**			**Remarks**	
	oil	**gas**	**water**	**oil**	**gas**	**water**		
Case 16	4.06	595	1.45	325	30650	14.5	$k_{rg(end\ point)}$ = 0.9	Stiff formation
Case 24	4.06	595	1.45	325	30695	14.5	$k_{rg(end\ point)}$ = 0.95	
Case 25	4.06	595	1.45	325	30738	14.5	$k_{rg(end\ point)}$ = 1	
Case 19	1.24	141	0.42	103	10173	5.73	$k_{rg(end\ point)}$ = 0.9	Medium formation
Case 26	1.24	141	0.42	103	10174	5.73	$k_{rg(end\ point)}$ = 0.95	
Case 27	1.24	141	0.42	103	10176	5.73	$k_{rg(end\ point)}$ = 1	
Case 22	0.76	79	0.26	64	6335	4.06	$k_{rg(end\ point)}$ = 0.9	Soft formation
Case 28	0.76	79	0.26	64	6335	4.06	$k_{rg(end\ point)}$ = 0.95	
Case 29	0.76	79	0.26	64	6335	4.06	$k_{rg(end\ point)}$ = 1	

5.3 Roles of Disconnected Secondary Fracture Networks

It is conceivable that secondary fractures, particularly those that are induced or re-opened during hydraulic fracturing, may close and become disconnected with the main hydraulic fracture upon shut-in and subsequent flow-back. It is unclear whether it is possible for the fracturing fluid to be trapped in the secondary fractures, or conversely, the secondary fractures could provide alternate pathways for the fluids to access the hydraulic fracture systems. In other words, how would these disconnected secondary fracture networks influence fracturing fluid recovery and oil production? Four specific cases (Cases A-D) are constructed to explore this issue (**Fig. 5.10**).

Case A – no secondary fractures;

Case B – all secondary fractures are oil-filled and disconnected with the hydraulic fracture. This corresponds to a scenario with naturally-occurring micro fractures;

Case C – secondary fractures are water-filled and disconnected with the hydraulic fracture. This corresponds to a scenario where induced fractures have lost contact with the main fracture;

Case D – a network of water-filled secondary fractures is partially connected to the hydraulic fracture. This corresponds to a scenario where induced micro fractures are located near the main hydraulic fracture.

The oil production profiles for these cases are compared in **Table 5.1**. The results underline the importance of secondary fractures in enhancing the overall conductivity of the system. It is clear that a system without any secondary fractures, either oil- or water-filled, has the worse production performance. The presence of either oil-filled or water-filled micro fractures, though disconnected directly from the main hydraulic fracture, could provide alternate pathways for

fluids to access the hydraulic fracture systems, which is reflected by the higher oil production observed in Cases B and C as compared to Case A. Finally, Case D yields the highest oil production, suggesting that water-filled secondary fractures do not necessarily act as barriers to oil flowing into the hydraulic fractures. In fact, counter-current imbibition between these water-filled secondary fractures, in addition to the presence of alternate pathways for fluids to flow towards the main hydraulic fracture, have contributed to the higher oil recovery.

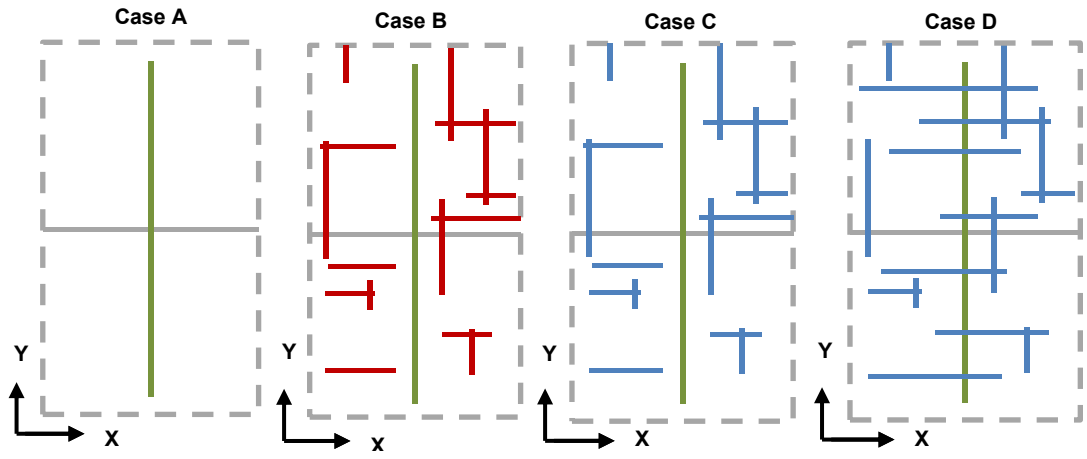

Fig. 5. 10 Illustration of fracture distribution for Cases A, B, C and D (Grey line = horizontal wellbore; green line = HF; blue line = water-filled NF; red line = oil-filled NF)

Chapter 6 Conclusions and Recommendations

In this study, we investigate water loss mechanisms and operational strategy during hydraulic fracturing flow back operation. Conclusions from this study and recommendations for future study are provided in this Chapter.

6.1 Conclusions

1. A numerical analysis is presented to understand the controlling factors of water retention, a phenomenon though commonly observed in unconventional wells, whose origin and understanding is a widely-debated subject among industry practitioners. A comprehensive sensitivity analysis on water-loss mechanisms during shut-in and flow-back is performed. The production profile from numerical result is compared with actual field data. Two particular mechanisms, including water retention/trapping in matrix and secondary fractures, are investigated. Higher initial rate does not necessarily imply enhanced long-term production. The recovery performance is the result of interplay between many factors such matrix/secondary fracture properties, matrix wettability, fracture compaction and shut-in duration. Uncertainties in secondary fracture parameters (length, intensity and connectivity) are assessed with a series of mechanistic models of stochastic discrete fracture networks.

2. Enlarged contact area between matrix and fracture enhances water imbibition into the matrix; therefore, water recovery decreases and oil production increases in both short and long terms.

3. Although the current thought in industry is that an extended shut-in may positively impact production performance, results from this study demonstrate that prolonged shut-in duration may benefit short-term oil production, but there is no observable improvement for long-term production. Due to the small volume of injected fracturing fluid, countercurrent imbibition is conceived to be limited to regions close the connected secondary fractures. On the other hand, lower bottom-hole pressure (more aggressive flow-back) is beneficial to water clean-up and long-term oil production in formation with high stiffness.

4. Desiccated matrix can reduce water recovery and oil production by decreasing its mobility.

5. Water transport depends on the interplay between viscous and capillary forces. Controlling factors including initial pressure distribution upon shut-in, secondary-fracture conductivity and matrix permeability are studied in terms of saturation and production profiles. A dimensionless capillary number N_{Ca} is formulated to describe their relative impacts: as N_{Ca} decreases, matrix imbibition increases, and water saturation in secondary fracture decreases at the end of shut-in, which is responsible for the decrease in water recovery.

6. Permeability jail in matrix can increase water saturation in secondary fractures, reducing oil production. It is suggested that reducing shut-in duration may mitigate this adverse influences.

7. This work presents an important insight in the role of secondary fracture in water loss. In contrast to some previous modeling studies, it illustrates the mechanisms and time-scales of

water retention in secondary fractures. In general, water is not permanently trapped, despite its potentially slow recovery.

8. Increasing capillary pressure and water relative permeability individually may improve imbibition; however, capillary pressure effect appears to be more dominant when the two factors are coupled. In general, imbibition enhances the initial oil production, but it also hinders water recovery. Long-term oil production is primarily influenced by oil relative permeability. To a certain extent, the impacts of capillary pressure and relative permeability would depend on the specific multiphase flow functions that are used. Therefore, a generalization of their combined impacts with initial water saturation would not be meaningful, as these factors are non-linearly related to wettability. Assessment regarding their impacts should be performed in a coupled manner by considering matrix wettability.

9. Fracture compaction can contribute to water loss in two ways: enhancing imbibition and reducing fracture conductivity. Reduction in fracture conductivity may reduce oil production; however, this negative impact can be counteracted by the benefits of improved counter-current imbibition. Matrix imbibition leads to more fracture compaction, which, in turn, enhances imbibition and water loss.

10. There are varying opinions among experts about the optimal flow-back strategy. Results from this study suggests that more aggressive flow-back is beneficial to water clean-up and long-term oil production in stiff rocks, while this benefit is less prominent in medium to soft

formation due to excessive fracture closure. Given that there is no direct correlation between high initial oil flow rate and improved cumulative oil production, in order to enhance the long-term production, measures for increasing oil relative permeability should be considered.

11. As the well bottom-hole pressure decreases below the bubble-point, gas production increases. The influence of gas relative permeability appears to be minimal; hence, only slight impact on the long-term gas production is noticeable, and this effect is the most obvious in stiff formations. In general, it is observed that any enhancement in gas production in medium to soft formations is often compromised by severe fracture closure.

12. This study presents an important insight regarding the roles of secondary fractures in unconventional reservoirs. Specifically, it helps to clarify the issue of whether disconnected secondary fractures are beneficial or detrimental to hydrocarbons recovery. Secondary fractures, though disconnected from the main hydraulic fracture, can still provide alternate pathways for fluids to access the hydraulic factures. Water-filled secondary fractures can also contribute to higher oil production by enhancing counter-current imbibition and overall conductivity of the entire system.

6.2 Recommendations

1. In addition to the tensile fractures, shear fractures are also propagating during hydraulic fracturing operation, which typically are not perpendicular with main artificial fracture. Fracture

network could be more heterogeneous when fractures are not perpendicular with each other, which could impact the flow back operation. Therefore, finite element method should be used to capture this non-perpendicular relationship between fractures and heterogeneity of fracture network.

2. During hydraulic fracturing operation, fractures propagate during injection period and fracture gradually close during shut-in and flow back period. Some fracture could lose contact with main hydraulic fracture. In order to evaluate this geomechanics effect on flow back operation, fully geomechanical model should be incorporated with fluid flow model to describe the process of fracture propagation and fracture closure, which could impact the water loss and flow back operation.

3. According to Nojabaei *et a*l. (2013), bubble-point pressure would decrease with formation pore radius reduction in tight rocks, indicating that tight rocks have different thermodynamic properties from conventional reservoirs, which could also impact water loss and flow back operation, therefore thermodynamic effect should be incorporated into the model in future.

Bibliography

Abbasi, M. A., Ezulike, D. O., Dehghanpour, H., and Hawkes, R. V. 2014. A Comparative Study of Flowback Rate and Pressure Transient Behavior in Multifractured Horizontal Wells Completed in Tight Gas and Oil Reservoirs. *Journal of Natural Gas Science and Engineering*, 17, 82-93.

Adefidipe, O. A., Xu, Y., Dehghanpour, H., and Virues, C. J. 2014. Estimating Effective Fracture Volume from Early-time Production Data: A Material Balance Approach. Paper SPE 171673 presented at the SPE/CSUR Uconventional Resources Conference, Calgary, Alberta, Canada, 30 September – 2 October.

Aguilera, R. 1980. *Naturally Fractured Reservoirs*. Petroleum Publishing Company.

Alahmadi, H.A.H. 2010. A Triple-Porosity Model for Fractured Horizontal Wells. MS thesis, Texas A&M University, College Station, Texas.

Alkouh, A., Mcketta, S., and Wattenbarger, R. A. 2014. Estimation of Effective-Fracture Volume Using Water-Flowback and Production Data for Shale-Gas Wells. *Journal of Canadian Petroleum Technology*, **53** (05), 290-303.

Almulhim, A., Alharthy, N., Tutuncu, A. N., and Kazemi, H. 2014. Impact of Imbibition Mechanism on Flowback Behavior: A Numerical Study. Presented at the Abu Dhabi International Petroleum Exhibition and Conference, Abu Dhabi, UAE, 10-13 November.

Alramahi, B. and Sundberg, M. I. 2012. Proppant Embedment and Conductivity of Hydraulic Fractures in Shales. Presented at the 46th US Rock Mechanics/Geomechanics Symposium, Chicago, IL, USA, 24-27 June.

Anderson, W. G. 1987. Wettability Literature Survey-Part 4: Effects of Wettability on Capillary Pressure. *Journal of Petroleum Technology* **39** (10): 1,283-1,300.

Anderson, W. G. 1987. Wettability Literature Survey-Part 5: The Effects of Wettability on Relative Permeability. *Journal of Petroleum Technology* **39** (11): 1,453-1,468.

Assiri. W. and Miskimins. J. L. 2014. The Water Blockage Effect on Desiccated Tight Gas Reservoir. Paper SPE 168160 persented at the SPE International Symposium and Exhibition on Formation Damage Control, Lafayette, Louisiana, USA, 26-28 February.

Aziz, K., and Settari, A. 1979. *Petroleum Reservoir Simulation*. Elsevier Applied Science Pub.

Baecher, G. B., Lanney, N. A., and Einstein, H. H. 1977. Statistical Description of Rock Properties and Sampling. Paper ARMA 77-0400 presented at The 18th U.S. Symposium on Rock Mechanics (USRMS), Golden, Colorado, USA, 22-24 June.

Bahrami, H. 2012. *Evaluating Factors Controlling Damage and Productivity in Tight Gas Reservoirs*. Curtin University.

Bazin, B., Peysson, Y., Lamy, F., Martin, F., Aubry, E., Chapuis, C. 2010. In-Situ Water-Blocking Measurements and Interpretation Related to Fracturing Operations in Tight Gas Reservoirs. *SPE Production & Operations* **25** (04): 431-437.

Bennion, D. B., Thomas, F. B., Schulmeister, B. E., and Ma, T. 2002. A Correaltion of Water and Gas-Oil Relative Permeability Properties for Various Western Canadian Sandstone and Carbonate Oil Producing Formations. Paper PETSOC-2002-066 presented at the Canadian International Petroleum Conference, Calgary, Alberta, Canada, 11-13 June.

Bennion, D. B., Thomas, F. B., Schulmeister, B. E., and Rushing, J. 2002. Laboratory and Field Validation of the Mechanism of Establishment of Very Low Initial Water Saturation in Ultra-low Permeability Porous Media. Paper PETSOC 2002-063 presented at Canadian International Petroleum Conference, Calgary, Alberta, Canada, 11-13 June.

Blair, P. M. 1960. Calculation of Oil Displacement by Countercurrent Water Imbibition. Presented at the Secondaty Recovery Conference, Wichita Falls, Texas, USA, 2-3 May.

Bradley, H. B. ed. 1992. *Petroleum Engineering Handbook*, third edition, Chap. 26. Richardson, Texas: SPE.

Brownscombe, E. R., and Dyes, A. B. 1952. Water-imbibition Displacement-a Possibility for the Spraberry. Paper API 52-383 presented at the Drilling and Production Practice, New York, USA, 1 January.

Cacas, M. C., Ledoux, E., Marsily, G. D., Tillie, B., Barbreau, A., Durand, E., Feuga, B., and Peaudecerf, P. 1990. Modeling Fracture Flow with a Stochastic Discrete Fracture Network: Calibration and Validation: 1. The Flow Model. *Water Resources Research* **26** (3): 479-489.

Cheng, Y. 2012. Impact of Water Dynamics in Fractures on the Performance of Hydraulically Fractured Wells in Gas-Shale Reservoirs. *Journal of Canadian Petroleum Technology* **51** (02): 143-151.

Chilès, J. P. 1988. Fractal and Geostatistical Methods for Modeling of a Fracture Network. *Mathematical Geology* **20** (6): 631-654.

Chilès, J. P. 2005. Stochastic Modeling of Natural Fractured Media: A Review. *Geostatistics Banff 2004*. Springer Netherlands. 284-294.

Cho, Y., Apaydin, O. G., and Ozkan, E. 2013. Pressure-Dependent Natural-Fracture Permeability in shale and Its Effect on Shale-Gas Well Production. *SPE Reservoir Evaluation & Engineering* 16 (02): 216-228.

Chu, L., Ye, P., Harmawan, I., Du, L. 2015. Characterizing and simulating the non-stationarity and non-linearity in unconventional oil reservoirs: Bakken application. *Journal of Unconventional Oil and Gas Resources* 9: 40-53.

Cil, M., Reis, J. C., Miller, M. A., and Misra, D. 1998. An Examination of Countercurrent Capillary Imbibition Recovery From Single Matrix Blocks and Recovery Predictions by Analytical Matrix/Fracture Transfer Functions. Paper SPE 49005 prepared for presentation at the SPE Annual Technical Conference and Exhibition, New Orleans, 27-30 September.

Clarkson, C. R., and Williams-Kovacs, J. D. 2013. Modeling Two-Phase Flowback of Multifractured Horizontal Wells Completed in Shale. *SPE Journal* **18** (04): 795-812.

Clemo, T. M. 1994. *Dual Permeability Modeling of Fractured Media*, University of British Columbia.

Computer Modeling Group. 2013. *IMEX: Three-phase, Black-oil Reservoir Simulator User's Guide (Version 2013)*. Computer Modeling Group Limited, Calgary, Alberta, Canada.

Coskuner, G. 2006. Completion Operations in Low Permeability Deep Basin Gas Reservoirs: To Use or Not to Use Aqueous Fluids, That is the Question. *Journal of Canadian Petroleum Technology* 45(10).

Crafton, J. W. 2008. Modeling Flowback Behavior or Flowback Equals "Slowback". Paper SPE 119894 presented at the SPE Shale Gas Production Conference, Fort Worth, Texas, USA, 16-18 November.

Crafton, J. W. 2010. Flowback Performance in Intensely Naturally Fractured Shale Gas Reservoirs. Paper SPE 131785 presented at SPE Unconventional Gas Conference, Pittsburgh, PA, USA, 23-25 February.

Crafton, J. W., and Noe, S. 2013. Impact of Delays and Shut-Ins on Well Productivity. Paper SPE 165705 presented at SPE Eastern Regional Meeting, Pittsburgh, Pennsylvania, USA, 20-22 August.

Dandekar, Abhijit Y. 2013. *Petroleum Reservoir Rock and Fluid Properties*. second edition. CRC Press.

Dutta. R., Lee, C., Odumabo, S., Ye, P., Walker, S. C., Karpyn, Z. T., Ayala H., L. F. 2014. Experimental Investigation of Fracturing-Fluid Migration Caused by Spontaneous Imbibition in Fractured Low-Permeability Sands. *SPE Reservoir Evaluation & Engineering* **17** (01): 74-81.

Economides, M. J., and Nolte, K. G. 2000. *Reservoir Stimulation*. Wiley.

Ehlig-Economides, C. A., Ahmed, I. A., Apiwathanasorn, S., Lightner, J. H., Song, B., Vera Rosales, F. E., Xue, H., and Zhang, Y. 2012. Stimulated Shale Volume Characterization: Multiwell Case Study from the Horn River Shale: II. Flow Perspective. Presented at SPE Annual Technical Conference and Exhibition, San Antonio, Texas, USA, 8-10 October.

Ertekin, T, Abou-Kassem, J.H. and King, G.R. 2001. *Basic Applied Reservoir Simulation*, SPE Textbook Series Vol. 7, Society of Petroleum Engineers.

Eskandari, K. and Srinivasan, S. 2010. Reservoir Modeling of Complex Geological Systems – a Multiple Point Perspective. *Journal of Canadian Petroleum Technology* **49** (8): 59-68.

Ezulike, D. O., Hawkes, R. V., and Dehghanpour, H. 2013. Understanding Flowback as a Transient 2-phase Displacement Process: An Extension of the Linear Dual-Porosity Model.

Paper SPE 167164 presented at the SPE Unconventional Resources Conference Canada, Calgary, Alberta, Canada, 5-7 November.

Ezulike, D. O., and Dehghanpour, H. 2014. Modelling Flowback as a Trasient Two-Phase Depletion Process. *Journal of Natural Gas Science and Engineering*. **19**: 258-278.

Fakcharoenphol, P., Torcuk, M. A., Wallace, J., Bertoncello, A., Kazemi, H., Wu, Y. S., and Honarpour, M. 2013. Managing Shut-in Time to Enhance Gas Flow Rate in Hydraulic Fractured Shale Reservoirs: A Simulation Study. Paper SPE 166098 presented at the SPE Annual Technical Conference and Exhibition, New Orleans, Louisiana, USA, 30 September.

Fakcharoenphol, P., Kurtoglu, B., Kazemi, H., Charoenwongsa, S., Wu, Y. 2014. The Effect of Osmotic Pressure on Improve Oil Recovery from Fractured Shale Formations. Paper SPE 168998 presented at the SPE Unconventional Resources Conference, The Woodlands, Texas, USA, 1-3 April.

Fan, L., Thompson, J. W., and Robinson, J. R. 2010. Understanding Gas Production Mechanism and Effectiveness of Well Stimulation in the Haynesville Shale Through Reservoir Simulation. Paper SPE 136696 presented at the Canadian Unconventional Resources & International Petroleum Conference, Calgary, Alberta, Canada, 19-21 October.

Firoozabadi, A., and Hauge, J. 1990. Capillary Pressure in Fractured Porous Media. *Journal of Petroleum Technology* **42** (06): 784-791.

Fisher, M. K., Wright, C. A., Davidson, B. M., Goodwin, A. K., Fielder, E. O., Buckler, W. S., Steinsberger, N. P., 2002. Integrating Fracture Mapping Technologies to Optimize Stimulations in the Barnett Shale. Paper SPE presented at the SPE Annual Technical Conference and Exhibition held in San Antonio, Texas, USA, 29 Sep-2 October.

Fjar, E., Holt, R. M., Raaen, A. M., Risnes, R., Horsrud, P., 2008. *Petroleum Related Rock Mechanics*, 2nd Edition, Elsevier.

Gale, J. E., Schaefer, R. A., Carpenter, A. B., and Herbert, A. 1991. Collection Analysis and Integration of Discrete Fracture Data from the Monterey Formation for Fractured Reservoir Simulations. Paper SPE 22741 presented at the SPE Annual Technical Conference and Exhibition, Dallas, Texas, USA, 6-9 October.

Gdanski, R. D., Fulton, D. D., Shen, C. 2009. Fracture-Face Skin Evolution During Cleanup. *SPE Production and Operations* **24** (01): 22-34.

Gdanski, R. D., and Walters, H. G. 2010. Impact of Fracture Conductivity and Matrix Relative Permeability on Load Recovery. Presented at SPE Annual Technical Conference and Exhibition, Florence, Italy, 19-22 September.

Ghanbari, E., Abbasi., M. A., Dehghanpour, H., Bearinger, D. 2013. Flowback Volumetric and Chemical Analysis for Evaluating Load Recovery and Its Impact on Early-Time Production. Paper SPE 167165 presented in SPE Unconventional Resources Conference-Canada, Calgary, Alberta, Canada, 5-7 November.

Ghanbari, E., Xu, M., Dehghanpour, H., Bearinger, D. 2014. Advances in Understanding Liquid Flow in Gas Shales. Paper SPE 171653 presented in SPE Unconventional Resources Conference-Canada, Calgary, Alberta, Canada, 30 September – 2 October.

Ghanbari, E., Dehghanpour, H. 2014. Impact of Rock Fabric on Water Imbibition and Salt Diffusion in Gas Shales. *International Journal of Coal Geology* **138** (2015): 55-67.

Ghanbari, E. 2015. *Water Imbibition and Salt Diffusion in Gas Shales: A Field and Laboratory Study*, University of Alberta.

Ghanbari, E., Dehghanpour, H. 2016. The Fate of Fracturing Water: A Field and Simulation Study. *Fuel* **163** (2016): 282-294.

Gupta, D. V. S. 2009. Unconventional Fracturing Fluids for Tight Gas Reservoirs. Paper SPE 119424 presented at the SPE Hydraulic Fracturing Technology Conference, Woodlands, Texas, USA, 19-21 January.

Holditch, S. A. 1979. Factors Affecting Water Blocking and Gas Flow from Hydraulically Fractured Gas Wells. *Journal of Petroleum Technology* **31** (12): 1515-1524.

Huo, D., Li, B., and Benson, S. M. 2014. Investigating Aperture-Based Stress-Dependent Permeability and Capillary Pressure in Rock Fractures. Presented at SPE Annual Technical Conference and Exhibition, Amsterdam, Netherlands, 27-29 October.

Jadhunandan, P. P., and Morrow, N. R., 1995. Effect of Wettability on Waterflood Recovery for Crude-Oil/Brine/Rock Systems. *SPE Reservoir Engineering* **10** (01): 40-46.

Jerauld, G. R. and Rathmell, J. J., 1997. Wettability and Relative Permeability of Prudhoe Bay: A Case Study in Mixed-Wet Reservoirs. *SPE Reservoir Engineering* **12** (01): 58-65.

Karimi-Fard, M., Durlofsky, L. J., and Azizm, K. 2004. An Efficient Discrete-fracture Model Applicable for General-purpose Reservoir Simulation. *SPE Journal* **9** (02): 227-236.

Karimaie, H., and Torsaeter, O. 2007. Effect of Injection Rate, Initial Water Saturation and Gravity on Water Injection in Slightly Water-Wet Fractured Porous Media. *Journal of Petroleum Science and Engineering*. **58** (2007): 293-308.

Kazemi, H., Merrill Jr., L. S., Porterfield, K. L., and Zeman, P. R. 1976. Numerical Simulation of Water-Oil Flow in Naturally Fractured Reservoirs. *SPE Journal* **16** (06): 317-326.

King, George. E. 2012. Hydraulic Fracturing 101: What Every Representative, Environmentalist, Regulator, Reporter, Investor, University Researcher, Neighbor, and Engineer Should Know About Hydraulic Fracturing Risk, *Journal of Petroleum Technology*. 64 (04): 34-42.

Lamson, B., Keith, D. Zotskine, Y., and Yule, K. D. 2013. An Unconventional Approach to a Conventional Field, How Slickwater has Changed the Game in the Cardium. Paper SPE 166268 presented at the SPE Annual Technical Conference and Exhibition, New Orleans, Louisiana, USA, 30 September-2 October.

Leverett, M. C. 1941. Capillary Behavior in Porous Solids. *Transactions of the AIME* **142** (01): 152-169.

Li, K., Chow, K., and Horne, R. N. 2006. Influence of Initial Water Saturation on Recovery by Spontaneous Imbibition in Gas/Water/Rock Systems and the Calculation of Relative Permeability. *SPE Reservoir Evaluation & Engineering* **9** (04): 295-301.

Li, K., Li, Y. 2014. Effect of Initial Water Saturation on Crude Oil Recovery and Water Cut in Water-Wet Reservoirs. *International Journal of Energy Research* **38**: 1599-1607.

Liang, T., Longoria, R. A., Lu, J., Nguyen, Q. P., and DiCarlo D. A. 2015. The Applicability of Surfactants on Enhancing the Productivity in Tight Formations. Paper SPE 178584/ URTeC 2154284 presented at the Unconventional Resources Technology Conference, San Antonio, Texas, USA, 20-22 July.

Liang, T., Longoria, R. A., Lu, J., Nguyen, Q. P., and DiCarlo D. A. 2015. Enhancing Hydrocarbon Permeability After Hydraulic Fracturing: Laboratory Evaluations of Shut-ins and Surfactant Additives. Paper SPE 175101 presented at the SPE Annual Technical Conference and Exhibition, Houston, Texas, USA, 28-30 September.

Long, J., Gilmour, P., and Witherspoon, P. A. 1985. A Model for Steady Fluid Flow in Random Three-dimensional Networks of Disc-shaped Fractures. *Water Resources Research* **21** (8): 1105-1115.

Longoria, R. A., Liang, T., Nguyen, Q. P., and DiCarlo D. A. 2015. When Less Flowback is More: A Mechanism of Permeability Damage and its Implications on the Application of EOR Techniques. Paper URTeC 2154266 presented at the Unconventional Resources Technology Conference, San Antonio, Texas, USA, 20-22 July.

Makhanov, K., Dehghanpour, H., and Kuru, E. 2012. An Experimental Study of Spontaneous Imbibition in Horn River Shales. Paper SPE 162650 presented at the SPE Canadian Unconventional Resources Conference, Calgary, Alberta, Canada, 30 October – 1 November.

Makhanov, K., Habibi, A., Dehghanpour, H., and Kuru, E. 2014. Liquid Uptake of Gas Shales: A Workflow to estimate Water Loss During Shut-in Periods after Fracturing Operations. *Journal of Unconventional Oil and Gas Resources* 7: 22-32

Mayerhofer, M. J., and Meehan, D. N. 1998. Waterfracs: Results From 50 Cotton Valley Wells. Paper SPE 49104 presented at the SPE Annual Technical Conference and Exhibition, New Orleans, Louisiana, 27-30 September.

McClure, M., and Zoback, M. D. 2013. Computational Investigation of Trends in Initial Shut-in Pressure during Multi-stage Hydraulic Stimulation in the Barnett Shale. Paper ARMA 2013-368 presented at the 47the U.S. Rock Mechaniscs/Geomechanics Symposium, San Francisco, California, USA, 23-26 June.

McClure, M. 2014. The Potential Effect of Network Complexity on Recovery of Injected Fluid Following Hydraulic Fracturing. Paper SPE 168991 presented at the SPE Unconventional Resources Conference, The Woodlands, Texas, USA, 1-3 April.

Morrow, N. R. and McCaffery, F. G. 1978. Displacement Studies in Uniformly Wetted Porous Media. Wetting, Spreading, and Adhesion, Academic Press, 289-319.

Nojabaei, B., Johns, R. T., Chu, L. 2013, Effect of Capillary Pressure on Fluid Density and Phase Behavior in Tight Rocks and Shales. *SPE Reservoir Evaluation & Engineering* 16(03): 281-289.

Osholake, T., Wang, J.Y., Ertekin, T. 2013, Factors Affecting Hydraulically Fractured Well Performance in the Marcellus Shale Gas Reservoirs. *Journal of Energy Resources Technology* **135.1**: 013402.

Pagels, M., Hinkel, J. J., and Willberg, D. M. 2012. Measuring Capillary Pressure Tells More Than Pretty Pictures. Paper SPE 151729 presented at the SPE International Symposium and Exhibition on Formation Damage Control, Lafayette, Louisiana, USA, 15-17 February.

Pak, A. 1997. *Numerical Modeling of Hydraulic Fracturing*. PhD Thesis. Edmonton, Alberta.

Parmar, J., Dehghanpour, H., and Kuru, E. 2012. Unstable Displacement: A Missing Factor in Fracturing Fluid Recovery. Paper SPE 162649 presented at the SPE Canadian Unconventional Resources Conference, Calgary, Alberta, Canada, 30 October – 1 November.

Parmar, J., Kuru, E., and Dehghanpour, H. 2013. Drainage Against Gravity: Factors Impacting the Load Recovery in Fractures. Paper SPE 164530 presented at the SPE Unconventional Resources Conference, The Woodlands, Texas, USA, 10-12 April.

Peters, Ekwere J. 2012. *Advanced Petrophysics*. Live Oak Book Company.

Pitman, J. K., Price, L. C., and LeFever, J. A. 2001. *Diagenesis and Fracture Development in the Bakken Formation, Williston Basin: Implications for Reservoir Quality in the Middle Member.* US Department of the Interior, US Geological Survey.

Pope, C., Benton, T., and Palisch, T. 2009. Haynesville Shale-One Operator's Approach to Well Completions in This Evolving Play. Presented at the SPE Annual Technical Conference and Exhibition, New Orleans, LA, USA, 4-7 October.

Purvis, R. A., and Bober, W. G. 1979. A Reserves Review of the Pembina Cardium Oil Pool. *Journal of Canadian Petroleum Technology* **18** (03).

Putra, E., Fidra, Y., and Schechter, D. S. 1999. Use of Experimental and Simulation Rsults for Estimating Critical and Optimum Water Injection Rates in Naturally Fractured Reservoirs. Paper SPE 56431 presented at SPE Annual Technical Conference and Exhibition, Houston, Texas, USA, 3-6 October.

Qasem, F. H., Nashawi, I. S., Gharbi, R., and Mir, M. I. 2008. Recovery Performance of Partially Fractured Reservoirs by Capillary Imbibition. *Journal of Petroleum Science and Engineering* **60** (1): 39-50.

Raghavan, R. and Chin L. Y. 2002. Productivity Changes in Reservoirs With Stress-Dependent Permeability. Paper SPE 77535 presented at the SPE Annual Technical Conference and Exhibition, San Antonio, Texas, USA, 29 Sep – 2 Oct.

Reinicke, A., Rybacki, E., Stanchits, S., Huenges, E., and Dresen, G. 2010. Hydraulic Fracturing Stimulation Techniques and Formation Damage Mechanisms—Implications from Laboratory Testing of Tight Sandstone–Proppant Systems. *Chemie Der Erde-Geochemistry* **70**: 107-117.

Rouleau, A. and Gale, J. E. 1985. Statistical Characterization of the Fracture System in the Stripa Granite, Sweden. *International Journal of Rock Mechanics and Mining Sciences & Geomechanics Abstracts* **22** (6): 353-367.

Rubin, B. 2010. Accurate Simulation of Non-Darcy Flow in Stimulated Fractured Shale Reservoirs. Paper SPE 132093 presented at the SPE Western Regional Meeting, Anaheim, California, USA, 27-29 May.

Shanley, K. W., Cluff, R. M., and Robinson, J. W. 2004. Factors Controlling Prolific Gas Production from Low-permeability Sandstone Reservoirs: Implications for Resource Assessment, Prospect Development, and Risk Analysis. *AAPG bulletin* **88** (8):1083-1121.

Sherman, J. B., and Holditch, S. A. 1991. Effect of Injected Fracture Fluids and Operating Procedures in Ultimate Gas Recovery. Presented at the SPE Gas Technology Symposium, Houston, Texas, USA, 22-24 January.

Sil, S. and Srinivasan, S. 2009. Stochastic Simulation of Fracture Strikes Using Seismic Anisotropy Induced Velocity Anomalies. *Exploration Geophysics* **40** (3).

Stone, H. L. 1973. Estimation of Three-Phase Relative Permeability and Residual Oil Data. *Journal of Canadian Petroleum Technology* **12**(04).

Stoyan, D., and Stoyan, H. 1994. *Fractals, Random Shapes, and Point Fields: Methods of Geometrical Statistics*. Chichester: Wiley.

Takahashi, S. and Kovscek, R. 2009. Spontaneous Countercurrent Imbibition and Forced Displacement Characteristics of Low-Permeability, Siliceous Shale Rocks. Presented at the SPE Western Regional Meeting, San Jose, California, USA, 24-26 March.

Tang, G., and Firoozabadi, A., 2001. Effect of Pressure Gradient and Initial Water Saturation on Water Injection in Water-Wet and Mixed-Wet Fractured Porous Media. *SPE Reservoir Evaluation &Engineering* **4** (06): 516-524.

Tong, Z., Xie, X., and Morrow, N. R. 2002. Scaling of Viscosity Ratio for Oil Recovery by Imbibition From Mixed-Wet Rocks. *Petrophysics* **43** (04).

Wang, M., and Leung, J. 2014. Investigating the Mechanisms and Time-Scale of Imbibition During Hydraulic Fracturing Flow-Back Operation in Tight Reservoirs. Paper presented at the International Discrete Fracture Network Engineering Conference, Vancouver, Canada, 19-22 October.

Wang, M., and Leung, J. 2015. Numerical Investigation of Fluid-Loss Mechanisms during Hydraulic Fracturing Flow-Back Operations in Tight Reservoirs. *Journal of Petroleum Science and Engineering* 133: 85-102.

Wang, M., and Leung, J. 2015. Numerical Investigation of Coupling Multiphase Flow and Geomechanical Effects on Water Loss During Hydraulic Fracturing Flow Back Operation. Unconventional Resources Technology Conference, San Antonio, TX, USA, 20-21 Jul.

Warren, J. E., and Root, P. J. 1963. The Behavior of Naturally Fractured Reservoirs. *SPE Journal* **3** (03): 245-255.

Wattenbarger, R. A., and Alkouh, A. B. 2013. New Advances in Shale Reservoir Analysis Using Flowback Data. Paper SPE 165721 presented at the SPE Eastern Regional Meeting, Pittsburgh, Pennsylvania, USA, 20-22 August.

Williams-Kovacs, J. D., and Clarkson, C. R. 2013. Stochastic Modeling of Two-Phase Flowback of Multi-Fractured Horizontal Wells to Estimate Hydraulic Fracture Properties and Forecast Production. Paper SPE 164550 presented at the Unconventional Resources Conference, Woodlands, Texas, USA, 10-12 April.

Woodland, D. C., and Bell, J. S. 1989. In Situ Stress Magnitudes from Mini-frac Records in Western Canada. *Journal of Canadian Petroleum Technology* **28** (05).

Xia, Y., Jin, Y., Chen, M., Chen, K., Lin, B., and Hou, B. 2014. Hydrodynamic Modeling of Mud Loss Controlled by the Coupling of Discrete Fracture and Matrix. *Journal of Petroleum Science and Engineering*.

Yu, W. and Sepehrnoori, K. 2014. Simulation of Gas Desorption and Geomechanisc Effects for Unconventional Gas Reservoirs. *Fuel* **116**: 455-464.

Yue, M., Leung, J., and Dehghanpour, H. 2013. Integration of Numerical Simulations for Uncertainty Analysis of Transient Flow Responses in Heterogeneous Tight Reservoirs. Paper SPE 167174 presented at the SPE Unconventional Resources Conference Canada, Calgary, Alberta, Canada, 5-7 November.

Zanganeh, B., Ahmadi, M., Hanks, C., and Awoleke, O. 2014. Proper Inclusion of Hydraulic Fracture and Unpropped Zone Conductivity and Fracturing Fluid Flowback in Single Shale Oil Well Simulation. Paper SPE 169511 presented at the SPE Western North American and Rocky Mountain Joint Regional Meeting, Denver, Colorado, USA, 16-18 April.

Zhou, X., Morrow, N. R., and Ma, S. 2000. Interrelationship of Wettability, Initial Water Saturation, Aging Time, and Oil Recovery by Spontaneous Imbibition and Waterflooding. *SPE Journal* **5** (2): 199-207.

Zolfaghari, A., Dehghanpour, H., Ghanbari, E., and Bearinger, D. 2015. Fracture Characterization Using Flowback Salt Concentration Transient. *SPE Journal*.

Zou, C. 2012. *Unconventional Petroleum Geology*, first edition, Newnes.